The effect of the mu-opioid receptor agonist DAMGO on neonatal rat astrocyte signalling and morphology.

Jack O'Brien-Cairney, BSc (Hons)

School of Life Sciences, University of Nottingham

Student Number: 4314557

Thesis submitted for the degree of Master of Research (MRes) in Neuroscience under the supervision of Dr Gareth Hathway and Dr Tomas Bellamy.

2017/2018 Academic Year

Word Count: 16,920

Contents

Table of Figures:

Abstract:

Astrocytes are known for modulating neuronal signalling in a plethora of different ways including the modulation of nociceptive signalling in the central nervous system. In recent years, work has been done to understand how astrocytic signalling is affected by different stimuli which would be released during pain responses.

The focus of this study was to observe whether mu-opioid receptor activation had any impact on the magnitude of calcium responses, the number of calcium spikes, or the percentage response rate of astrocytes that had been treated with either 1µM ATP or 100nM SP; and whether mu-opioid receptor activation had any effect on forskolin-induced stellation of astrocytes.

Astrocytes were cultured from sacrificed P2 Wistar rats and were loaded with a calcium indicator dye called Fluo-5F AM. The changes in fluorescence intensity expressed by the astrocytes following stimulation with 1uM ATP or 100nM substance P (SP) in the absence and presence of DAMGO ([D-Ala2, N-MePhe4, Gly-ol]-enkephalin) were measured and compared against each other. Cortical astrocytes were incubated both under control conditions and with 10µM DAMGO in the presence and absence of 100µM forskolin for three hours at 37°C prior to being fixed using a 4% PFA solution. The prevalence of stellate morphology was manually assessed and compared using both Kruskal-Wallis and Mann-Whitney statistical tests.

The results of this study show that DAMGO reduces the magnitude of calcium responses (from 2.51-fold to 1.36-fold higher than baseline; $p<0.0001$) and response rate (from 84.62% to 44.60%; $p<0.0001$) of ATP-treated spinal astrocytes. However, these changes are not found among ATP-treated cortical astrocytes. Similarly, DAMGO appears to have no significant effect on the magnitude or number of calcium responses produced by SP binding among both spinal and cortical astrocytes. However, secondary applications of SP alone significantly reduced calcium response magnitudes among spinal astrocytes (from 2.48-fold to 1.26-fold higher than baseline; $p = 0.0009$). These results suggest that initial binding of SP causes astrocytes to become desensitised to further SP-induced calcium activity.

Chronic (3h) exposure of cortical astrocytes to DAMGO at 37°C and at 5% CO_2 had no significant effect on the prevalence of stellate cells compared to those fixed under control conditions ($p>0.99$). Chronic exposure to a single application of DAMGO and forskolin also did not significantly change the prevalence of stellate cells among those that were treated with solely forksolin for three hours ($p>0.99$). These results suggest that chronic exposure to a single application of DAMGO has no significant impact on astrocyte morphology.

Aims:

Recent work has suggested that the functionality of astrocytes in the central nervous system changes between neonates and adults. The aims of this study were to observe whether opioidergic signalling, using DAMGO, had any role in affecting signalling among neonatal astrocytes and whether DAMGO had any impact on the morphology of cultured astrocytes e.g. in stellation. The hypothesis of this study is that opioidergic signalling using the mu-opioid receptor agonist DAMGO will inhibit gliotransmitter-induced signalling and inhibit morphological changes.

Introduction:

Humans have the ability to process, cognitively, the sensation of pain rather than solely react to noxious stimuli. The official definition of pain is an unpleasant sensory and emotional experience associated with actual or potential tissue damage, or described in terms of such damage (Merskey et al., 1979).

The biological importance of pain has led to the research field expanding as scientists and clinicians alike wish to answer novel and crucial questions about pain. For example, although research has shown how painful sensations are relayed throughout the body, scientists are still uncertain about how these pain signals are fully modulated, how they vary biologically between neonates and adults, how pain persists after the noxious stimulus is no longer present, and other such questions. The

answers to these questions have been increasingly sought after as our understanding of pain has become more comprehensive.

Primary afferent fibres:

Noxious stimuli, whether they be; thermal, mechanical, or chemical, excite the peripheral ends of nociceptors, which are a subset of a population of neurons called primary afferent fibres which extend toward the dorsal horn of the spinal cord and terminate within the laminae of the dorsal horn (Basbaum and Jessell, 2000). These afferent fibres which extend from the target organs to the dorsal horn of the spinal cord are comprised of four subspecies which are the Aα, Aß, Aδ, and C fibres though the Aα and Aß fibres are responsible for the detection of innocuous touch whereas the Aδ and C fibres are classified as nociceptors and carry pain signals to the dorsal horn (Meyer et al., 2008). The three species of A-fibre are all myelinated, however, the Aα and Aß have significantly larger diameters than the Aδ fibres which are responsible for mediating well-localised, acute pain (Meyer et al., 2008). The C fibres are the second class of nociceptor, according to Meyer, as they convey poorly-localised pain at a slower conduction velocity due to being unmyelinated (Bessou and Perl, 1969; Meyer et al., 2008).

The nociceptors, Aδ and C fibres, are heterogeneous (Snider and McMahon, 1998; Perl, 2007; Meyer et al., 2008). There are two types of Aδ fibres; type I Aδ fibres which have a low mechanical and chemical threshold but a high heat threshold (above 50°C) and would therefore mediate acute pain that was induced by noxious mechanical stimuli, and

type II Aδ fibres which have a lower thermal threshold but high mechanical thresholds, and mediate acute pain in response to noxious heat (Meyer et al., 2008).

C fibres on the other hand, can be either polymodal in that they can respond to multiple different types of stimuli, much like the myelinated afferent fibres, and exist in both heat-sensitive and mechanically-sensitive subpopulations (Perl, 2007). C fibres can be characterised by what they release upon stimulation (Snider and McMahon, 1998). There are two categories of C fibre which are called peptidergic and non-peptidergic C fibres which can be differentiated by both their receptor expression profiles and where they terminate within the dorsal horn of the spinal cord (Snider and McMahon, 1998; Dong et al., 2001). Those C fibres that are peptidergic are known to release neuropeptides such as substance P and calcitonin-gene related protein, and are responsive to nerve growth factor (NGF) due to expressing TrkA neurotrophin receptors, however, nonpeptidergic C fibres are devoid of neuropeptides, and express c-Ret neurotrophin receptors that are targeted by glial-derived neurotrophic factor (GDNF) (Hunt and Rossi, 1985; Dong et al., 2001). A significant number of the c-Ret-positive nociceptors also express specific subtypes of purinergic receptors, most notably the ATP-gated $P2X_3$ receptors (Vulchanova et al., 1998).

The primary afferent fibres terminate in the dorsal horn which is comprised of laminae that are anatomically and electrophysiologically distinct (Basbaum and Jessell, 2000) (Figure 1).

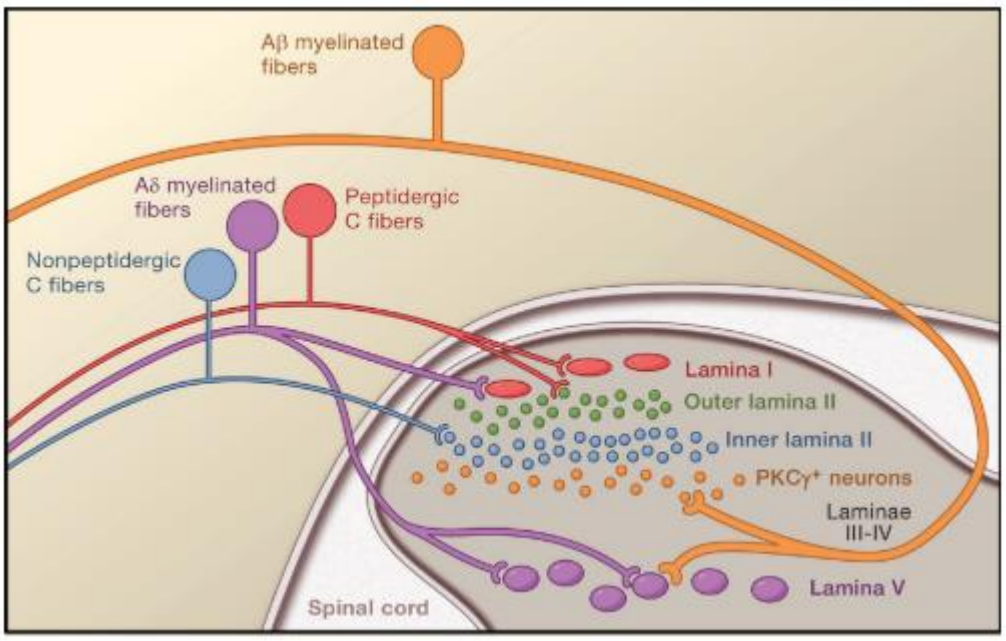

Figure 1: The organisation of connections made between primary afferent fibres and the dorsal horn of the spinal cord. The unmyelinated non-peptidergic C (shown in red) and myelinated Aδ fibres (shown in purple) terminate in the most superficial laminae, lamina I and the outer portion of lamina II, where they synapse with large projection neurons (shown in red) and interneurons (shown in green). The non-peptidergic C fibres (shown in blue), however, project to the deeper inner lamina II where they synapse with interneurons (shown in blue). Signals induced by innocuous stimuli which are carried by Aß fibres (shown in orange) are sent to neurons in the ventral part of lamina II that express protein kinase C gamma (PKCγ¬+) (also shown in orange). Innocuous and noxious input is carried by Aß and Aδ fibres respectively to lamina V (shown in purple). (From ((Basbaum et al., 2009)*).*

Those afferent fibres that convey information related to innocuous stimuli such as the Aß fibres terminate in lamina V which is deep within the dorsal horn whereas nociceptors terminate in more superficial laminae such as lamina I in the case of peptidergic C fibres and both the inner and outer sections of lamina II in the case of non-peptidergic C fibres and some Aδ fibres. Both the peripheral and central terminals of

primary afferent fibres have been targets for pain medications due to being the immediate propagators of nociceptive signals. Though opium has been used for pain relief for millennia and its use in surgeries has been recorded for many centuries (Norn et al., 2005), our understanding of how opioids (both natural and synthetic) work to produce antinociceptive effects only strengthened over recent decades. Opioids act on the peripheral terminals of primary afferent fibres and cause the inhibition of action potential production in response to noxious stimuli, therefore, leading to a reduction in pain signalling (Kumamoto et al., 2011). A number of studies have shown that among primary afferent fibres there are synergistic interactions between opioid receptors and neurotransmitter receptors, for example, δ-opioid receptors interact with α_{2A} adrenoceptors. These interactions cause the inhibition of glutamatergic transmission among substantia gelatinosa (SG) neurons (Kawasaki et al., 2003). The research done on primary afferent fibres and analgesics gave rise to further research regarding the effects of analgesics on sensory neurons throughout the CNS, particularly in regard to the ascending and descending control of pain.

How nociceptors develop in vivo:

The sensory neurons that are classified as nociceptors develop from migratory neural crest cells that move from the dorsal section of the neural tube. Neurons, specifically those that go on to become low-threshold mechanoreceptors and proprioceptors, are born at an earlier point in neurogenesis when compared to the nociceptor lineage whose members are born at a later stage (Anderson, 2000).

Neurogenin 1 (Ngn1) is expressed by developing neurons. Ngn1 allows for the expression of TrkA, TrkB, and TrkC: the formermost is expressed by newly developing embryonic nociceptors (Marmigère and Ernfors, 2007) whereas the latter two compounds are expressed in some species of low-threshold mechanoreceptors (Ma et al., 1998, 1999). The zinc finger protein Klf7 and the homeobox gene Brn3a are not directly required for the activation of TrkA but rather are necessary for the maintenance of the TrkA protein.

After the early stages of sensory neurogenesis, the proto-nociceptors are driven down two distinct developmental pathways that ultimately result in the formation of two classes of nociceptors: peptidergic and nonpeptidergic nociceptors. Immediately preceding the birth of the individual and during the postnatal period, a portion of the developing cells switch off their expression of TrkA and begin to express a transmembrane signalling component of the glial cell-derived growth factor receptor (GDNF) called Ret (Luo et al., 2007). These cells become non-peptidergic cells that bind isolectin B4 (IB4). The remaining cells that continued to express TrkA develop into peptidergic nociceptors that exhibit calcitonin gene-related protein (CGRP) and substance P (SP) but do not bind IB4 (Bennett et al., 1996; Molliver et al., 1997). Early embryonic nociceptors share a fairly similar molecular makeup, as they co-express both TrkA and Runx1. However, during the segregation process the expression balance between TrkA and Runx1 shifts such that Runx1 is downregulated to favour TrkA expression in peptidergic nociceptors. Conversely, the non-peptidergic nociceptors that bind IB4

continue to express Runx1 but cease to express TrkA, as previously stated. Conditionally knocking-out the expression of the Runx1 gene causes the developing cells to transform into TrkA+ CGRP+ type i.e. peptidergic nociceptors (Chen et al., 2006; Yoshikawa et al., 2007). On the other hand, the potentiated expression of the Runx1 gene in developing nociceptors inhibits the development of peptidergic nociceptors (Kramer et al., 2006).

Astrocytes, which are intimately coupled with both afferent and efferent sensory neurons, develop from gliogenic radial glia though whether or not different subtypes of astrocytes develop from later evolutions of gliogenic radial glia remains unclear though an increasing bank of data certainly shows that astrocytes continue to develop throughout embryological development and change morphology and function through postnatal fine-tuning through to adulthood (Bayraktar et al., 2015). Much work has been done recently in order to thoroughly understand the spatiotemporal heterogeneity of astrocytes. For example, it has been shown different regions of the adult human brain possess different astrocyte expression profiles whereby throughout the brain the functionality, receptor expression, and reactivity vary (Bachoo et al., 2004; Oberheim et al., 2006).

Astrocytic structure and signalling:

Astrocytes are a subspecies of glial cell that were first identified around 150 years ago, and were first only considered to be involved in supporting the metabolic and structural integrity of neuronal networks within the brain and spinal cord (Bowman and Kimelberg, 1984; Nag,

2011). For example, astrocytes are known for supplying neurons with energy via glucose through the GLUT1 transporter present on the astrocytes' surfaces, and oxygen through the cellular processes that make contact with the walls of blood vessels because this eliminates the need for a more mosaic-like structure of the blood-brain-barrier (Morgello et al., 1995)**.**

At the level of the synapse, however, it is important to note that astrocytes send out processes that connect to many pairs of synapses but each component of this collective superstructure are referred to as a tripartite synapse (Gray, 1959; Araque et al., 1999). Cortical astrocytes also express significant regional morphological heterogeneity. In African giant rats (*Cricetomys gambianus)*, for example, it was observed that the brain stem and corpus callosum were predominantly populated with fibrous astrocytes whereas the areas of the cortex and dentate gyrus were occupied by protoplasmic astrocytes (Olude et al., 2015). Olude et al also observed that the diameter of astrocytic somas, expression density, and the GFAP staining intensity of astrocytes were age-dependent, and that changing densities of astrocytes are postulated to be either a response to neuronal damage resulting from ageing or that they are important in maintaining a similar level of neuroprotection that would be present in a neonatal animal.

Astrocytes are unable to produce action potentials and are, therefore, not able to communicate through electrical signals. Instead, they communicate via excitations resulting from changes in their intracellular calcium ion concentration (Cornell-Bell et al., 1990). These

elevations can both occur spontaneously (Parri et al., 2001; Nett et al., 2002; Hirase et al., 2004) and be directly evoked in response to pharmacological and or physiological stimulation (Dani et al., 1992). The release of Ca^{2+} from endoplasmic reticula is generally mediated by inositol 1,4,5 triphosphate (IP_3) produced via the activation of G-protein-coupled receptors through neurotransmitter binding such as with ATP (Jeremic et al., 2001). Knock-out studies have shown that extracellular ATP, which would be released by sensory neurons in vivo, predominantly evokes calcium responses in astrocytes via both the metabotropic P2Y1 and the ionotropic P2X7 receptors (Hamilton et al., 2008). However, the expression of other subtypes of P2X receptor, which still bind ATP, is affected under pathological conditions; for example, in cases of inflammatory and neuropathic pain (Kage et al., 2002; Xu and Huang, 2002). As a result of P2X receptor expression being affected by inflammation and neuronal damage, P2X receptors and ATP activity have become a source of focus with regard to pain treatment.

There is a functional coupling of mu-opioid receptor agonists with the activity of P2X receptors in sensory neurons. Sensory neurons respond to ATP in a manner which consists of a fast and slow current which are mediated by P2X3 receptors and heterodimeric P2X2/3 and P2X2 receptors respectively, and both of these evoked currents are inhibited by the activity of mu-opioid receptor agonists (Chizhmakov et al., 2005). The effect of mu-opioid receptor agonists on ATP-induced activity in sensory neurons which are functionally coupled with astrocytes that are themselves sensitive to ATP shows that investigating if and how

astrocytes are affected by mu-opioid receptor activity may give rise to valuable insights into how pain signals are mediated.

Opioid receptor structure:

Opioid receptors are a class of membrane-bound structures that belongs to large group of G-protein-coupled receptors (GPCRs), which are the most prevalent form of receptors on cellular surfaces, and act as targets for approximately one-third of drugs available on the market (Vortherms and Roth, 2005). At a fundamental level, GPCRs can be classified by their expression of seven transmembrane domains consisting of alpha-helical segments that are divided by interlacing intra- and extracellular loops (Fredriksson et al., 2003). Due to their prevalence in numerous bodily environments including; the components of the central nervous system, and the gastrointestinal tract, opioid receptors are heavily studied in numerous fields but particularly in pain modulation (Pasternak, 2014)**.** Opioid receptors come in three primary flavours: δ−opioid, μ−opioid, and κ−opioid receptors that were all originally crystallised in their respective inactive states in which they were bound to an antagonist; these were naltrindole (Granier et al., 2012), beta-funaltrexamine (Zimmerman et al., 1987), and JTDic (Wu et al., 2012). Endomorphins, enkephalins, and dynnorphins among other naturally occurring peptides and or alkaloids are common activators of these opioid receptors (Piestrzeniewicz et al., 2006).

The primary binding site of most GPCRs is enveloped deep within the structure of the receptor, in particular, it is submerged within the bundle of helices between the superficial components of the

transmembrane domains and the second extracellular loop (ECL2). Some notable examples of this structural archetype would be the M2 and M3 muscarinic receptors for which a layer of tyrosine residues covers the ligand binding-site (Haga et al., 2012; Kruse et al., 2012). The binding site (also referred to as a binding pocket due to its partially submerged structure) for β-FNA in the μ-opioid receptor (μOR) is mostly exposed to ligands from the extracellular surface (Manglik et al., 2012). The increased extracellular exposure of the μOR's binding pocket has been suggested as a reason for the increase in rapidness of opioid half-lives; for example, alvimopan has a half-life of 30 minutes when bound to the μOR (Cassel et al., 2005) whereas, due to the aforementioned cloaking of the muscarinic binding site through tyrosine residues, the half-life of the drug tiotropium at the M_3R is 34.7 hours (Disse et al., 1993).

For the mu opioid receptor in particular a region within the third extracellular loop to the C terminus was determined to be crucial for establishing the selectivity towards agonists whereas the selectivity towards antagonists is primarily determined by an alternative region of the receptor (Xue et al., 1995).

How pain signals are modulated:

Pain signals are controlled, whether by facilitation or inhibition, in a bidirectional manner triggered by the activation of sites within the midbrain and medulla. The first region of the brain to be demonstrated, explicitly, to induce inhibition of endogenous pain signals was the periaqueductal gray (PAG); in which a profound antinociceptive response

was observed following microinjections of opioids in both animals (Reynolds, 1969) and humans (Hosobuchi et al., 1977). The PAG receives input from sites within the cortex as well as nociceptive inputs from the dorsal horns of spinal vertebrae via the parabrachial nuclei (Gauriau and Bernard, 2002).

The influence of the PAG on descending pain modulation is governed primarily through its bidirectional connections with the rostroventomedial medulla (RVM). This was demonstrated in a 1979 study which revealed that activation of PAG neurons, through both electrical and chemical stimulation (morphine), was closely associated with neuronal activation in the RVM (Behbehani and Fields, 1979).

The RVM, on the other hand, is composed of numerous substructures containing clusters of neurons (nuclei) which includes the nucleus raphe magnus (NRM) which is predominantly serotonergic in nature; alongside the NRM, the nucleus reticularis gigantocellularis-pars alpha and the nucleus paragiganto-ccellularis lateralis (Vanegas and Schaible, 2004) are also included in the grand structure of the RVM. As previously stated, the PAG receives input from cortical and midbrain sites, however, the RVM receives input from different supraspinal regions including the thalamus, the locus coeruleus, and the parabrachial region. Due to its functional connections and associations with the PAG, the RVM is often considered to be the ultimate common relay in regards to the descending control of pain signalling, as it projects signals to both the dorsal horns of spinal vertebrae and the trigeminal nucleus caudalis (Vanegas and Schaible, 2004; Heinricher et al., 2009). The RVM is also

somewhat unique functionally in regards to pain modulation as it is able to exert both negative (inhibitory) and positive (facilitatory) effects on nociceptive signals being detected - this was initially discovered through the identification of “on-cells” and “off-cells” which demonstrated an increase in their activity in response to noxious stimuli and or prior to behavioural output, and a cessation of activity prior to tail-flicks respectively (Vanegas and Schaible, 2004; Heinricher et al., 2009). This, therefore, gave rise to the insight of opioid function in regards to pain modulation in that they triggered the cessation of on-cell activity and the facilitation of off-cell activity, meaning that there was an increase in the activity of cells that produced inhibitory effects thereby producing a greater degree of inhibition overall. This mechanism was later deemed necessary and sufficient to produce analgesia (Heinricher et al., 2009). Since, the sites involved in the descending control of pain receive input from higher cortical areas of the brain, it could be said that the control of pain, although normally controlled by a purely cellular or physiological system, can also be augmented and influenced by external and more conscious input (Heinricher et al., 2009), however, the extent to which humans can “will away pain” through conscious thought is not clearly known as it varies both among individuals and across time for each individual.

Many studies that involve animal models of both neuropathic and inflammatory pain have supported the view that imbalances between the facilitatory and inhibitory systems of descending pain control underlie the progression and development of numerous pathological pain states. On-

cell activity in the RVM is enhanced in response to injury and or inflammation; alongside this, disruption of the descending facilitation from the RVM through pharmacological, neurochemical, or physical means has resulted in the abolition of enhanced behavioural responses to noxious stimulation without the attenuation of acute, protective reflexes (Gardell et al., 2003; Bee and Dickenson, 2007). In the instance of migraine, however, work has been done more recently through which microinjection of anaesthetics into the RVM has been shown to alleviate ongoing pain symptoms in animal models, and that similar results could also be attained for neuropathic pain (King et al., 2009; De Felice et al., 2013).

It is important to note that the neurobiology of pain processing varies progressively between neonates and adults, and that noxious stimulation during this period of neuroplasticity can cause unpredicted epigenomic changes which lead to long-term changes in the brain including changes to pain sensitivity and reactivity in adulthood (Eckstein Grunau, 2013). During early life, the neonatal spinal cord acts as an independent unit and as the descending pathway is still immature (Fitzgerald, 1991), the neonatal cortex does not exert as much control over pain processes as it would do in the adult (Fitzgerald, 1993). Within the dorsal horn of the neonatal spinal cord, there is an increase in NMDA receptor expression which through accentuating the low pain threshold of the neonate increases the vulnerability of the newborn brain (Kim et al., 1996). The analgesia evoked by PAG stimulation does not become effective until P21 in rats as the immature analgesic system is unable to

diminish noxious inputs entering the CNS meaning that their effects are more profound in infants than in adults (van Praag and Frenk, 1991). Both anatomical differences between the adult and neonatal CNS and functional differences such as how the inhibitory effect of GABA in adults is inversed in neonates as GABA induces depolarisation in a manner partly dependent on intracellular chloride concentrations (Ben-Ari et al., 2012) have provided insight into why age is an important factor to consider when researching the biology and new treatments of pain. However, much work has been primarily focused on the effects of pain treatment, including opioids, on sensory neurons therefore, given the importance of astrocytes and other glial cells in regulating the activity of sensory neurons, investigating the effects of analgesics on astrocyte function would be beneficial to advancing our understanding of how pain treatments work.

Opioid receptors in pain, and astrocytic, signalling:

Astrocytes make numerous contributions to the overall manner which neuronal signalling occurs in the central nervous system. They do this, primarily, by releasing various gliotransmitters at different stages of synaptogenesis including both presynaptic and postsynaptic development, the maintenance of the extracellular environment and functionality of cells, and the plasticity of signalling patterns (Ben Achour et al., 2010; Haydon and Nedergaard, 2014). Thrombospondins (TSPs) are known to promote synaptic formation in vivo as well as in vitro, however, they exhibit a seemingly reciprocal relationship with tumor

growth factor beta (TGFB) in astrocytes despite TGFB inducing excitatory synapses via a mostly d-serine dependent mechanism (Christopherson et al., 2005)

A recent study demonstrated that microinjections of oxytocin into the ventrolateral orbital cortex (VLOC) attenuate neuropathic pain and it was suggested that some species of opioid receptor present in the VLOC contribute to the antiallodynic effect of the injection of oxytocin into the VLOC (Taati and Tamaddonfard, 2018).This effect was demonstrated by the increased paw withdrawal threshold (PWT) in response to 5, 10, and 20ng per site dosages of oxytocin, however, the antiallodynia that would have been produced by the oxytocin was inhibited by a prior injection of atosiban (100ng/site) and naloxone (500ng/site) which are antagonists of oxytocin receptors and opioid receptors respectively (Taati and Tamaddonfard, 2018)**.**

After breeding mice which expressed Cre-recombinase under the promoter for the sodium channel type Nav1.8 with mu opioid receptor (MOR)-floxed mice, the offspring were subject to paw injections to see whether the mu opioid receptors were indeed the receptor species present on the surface of the primary nociceptive afferents (Severino et al., 2018)**.** Using the MOR agonist DAMGO, the conductors of the study noticed that the levels of substance P release was lower in flMOR mice when compared to the heterogeneous individuals as a result of inhibition; this provided evidence that there was indeed a loss of opioid receptor function at the terminals of the central afferents which suggested that

MORs play a role in mediating hyperalgesia and in remitting the symptoms of chronic pain states (Severino et al., 2018).

It has been previously shown that responses to anti-nociceptive drugs made by kappa opioid receptors (KORs) exhibit an inverted U-shape, specifically for peripherally-restricted nociceptors exposed to U50488, and that the downward phase of the response could be blocked via the use of an ERK inhibitor called U0126 (Jamshidi et al., 2015). Jamshidi and others administered a KOR agonist called salvinorin A (Sal-A) to observe its effects on the opioid receptor's response and they noted that although the characteristic shape of the curve was conserved, the downward phase was not affected in the same way when using Sal-A in contrast to U50488. However, the dose-response curve concerning Sal-A was affected by partial inhibition of c-Jun N-terminal kinase (JNK). Jamshidi and others commented that they found that adenylyl cyclase (AC) activity within the nociceptor had been affected by both conditions with similar efficacies but that the difference was in their approach; the binding of U50488 resulted in the reduction in AC activity through the activation of the ERK pathway whereas the Sal-A binding gathered its effect through JNK activation (Jamshidi et al., 2015).

Chronic exposure to opioids changes the manner in which delta-opioid receptors among others are trafficked to the membrane of the astrocytes. Though it has been shown that the inhibition of either the entry of extracellular calcium or the activity of intracellular IP_3 triggers a significant decrease in the internalisation of delta-opioid receptors, this occurs in tandem with the potentiating effects of intracellular ATP and

depolarisation induced by high potassium concentrations within the cell ergo the exact role of intracellular calcium in modulating the morphology or functionality of opioid receptors is unclear (Bao et al., 2003).

Methodology:

Ethical Approval:

Animals were humanely killed by cervical dislocation and decapitation in accordance with the policies on the care and use of laboratory animals of British Home Office and European Community Laws. The University of Nottingham Animal Welfare and Ethical Review Body approved of the experiments which used the Wistar rats supplied by Charles River Laboratories UK, Ltd.

Tissue collection:

Male and female Wistar rats (Charles River UK Ltd, UK) were sacrificed, at postnatal day two (P2), by decapitation after cervical dislocation. The heads and spinal cord were removed from the animal using dissection scissors, scalpels, and forceps that had been heated the day prior to ensure sterile conditions, and were then placed in ice-cold dissection buffer which contained: 25ml of 10X Hank's Balanced Salt Solution (HBSS) (Thermo-Fisher, UK), 225ml of distilled water, and one aliquot of a glucose-penicillin-streptomycin (GSP) mixture which contained one aliquot of penicillin-streptomycin (Thermo-Fisher, UK), 0.99g of glucose (Thermo-Fisher, UK), and 1.19g 4-(2-hydroxyethyl)-1-piperazineethanesulfonic acid (HEPES) (Sigma-Aldrich, Gillington, UK). The dissection buffer was adjusted to a pH of 7.2 using drop-wise NaOH.

The skulls and meninges of the neonate were removed using sterile scalpels, and the remaining tissue (cerebella and spinal cord) were then transferred to a petri dish filled with dissection buffer. A dropper was used to remove the buffer from the tissue and to replace it with buffer containing 5ml of papain (Sigma-Aldrich, Gillington, UK). The tissue was then cut into smaller pieces using a sterile blade. The tissue was then covered with foil and incubated at 37°C for 40 minutes.

500ml of glial medium was produced by combining 450ml of Dulbecco's Modified Eagle's Medium (DMEM) (Sigma-Aldrich, Gillington, UK), 50ml of foetal bovine serum (FBS), one aliquot of penicillin-streptomycin, and 25mg of proline. This medium was sterilely filtered into a vacuum flask and incubated at 37°C.

20ml of poly-l-lysine was produced in distilled water and was filtered with a sterile syringe. The 22mm coverslips were then distributed among six-well plates, and then had 500µL of poly-l-lysine solution applied to them. The coverslips were then left for 30 minutes.

After the tissue had incubated for 40 minutes, 0.5ml of DNase solution was applied to the tissue. The tissue was then transferred to a 15ml falcon tube and was spun at 212g for 6 minutes in a centrifuge. After six minutes had passed, the supernatant was drawn off and replaced with approximately 2mL of glial medium and an addition 0.5mL of DNase solution, and the tissue solution was titrated using a 1-bore Pasteur pipette for 20 cycles. The tissue solution was then centrifuged at 182g for a further three minutes. The supernatant was then collected and titrated

in 10mL of glial medium, after which it was again centrifuged at 182g for three minutes. The previous step was performed twice. The final centrifugation was performed at 212g for 6 minutes, after which the supernatant was poured off and the pellet was re-suspended in 10mL of glial medium. The suspended pellet was then strained through a 100µm cut-off cell-strainer, and the cell density was measured using a haemocytometer.

The poly-l-lysine was then aspirated from the coverslips and replaced with a 1mL glial medium wash which was then aspirated from the coverslips. After this, an appropriate volume of cell suspension was applied to each coverslip to produce the desired cell density of 2.5x104 cells per mL, as well as 2mL of glial medium per well. This glial medium was replaced firstly, after 24 hours, and then after every 3-4 days. The astrocytes were ready for use in calcium imaging and bright-field imaging experiments after 7-10 days as this time period allowed the astrocytes to mature to an appropriate state for use in experiments.

Drug Preparation:

The fluorescent dye used in these experiments was Alexa Fluora 5 FAM (Invitrogen, UK) at a stock concentration of 100uM made from dissolving 50ug of the dye in solid form in 454uL of pluronic vehicle which required the solution to be vortexed at 1600-3000rpm for approximately five minutes. This solution was the aliquoted into 35uL samples (to provide ample excess) and stored at -20 degrees Celsius. For use in the experiments, 30uL of the dye solution was added to 3ml of imaging buffer solution, creating a final concentration of 0.990099 (~1) uM in solution.

The basic imaging buffer was made by dissolving 7.8894g NaCl (Fisher), 0.2237g KCl (Fisher), 2.3830g HEPES (Sigma), and 2.7023g of anhydrous glucose (Fisher) in one litre of distilled water producing final concentrations of 135mM, 3mM, 10mM, and 15mM respectively. The solution was then pH calibrated by adding 10M NaOH in a dropwise fashion until the pH of the solution reached 7.4 and had stabilised around this value. This solution was stored at 4 degrees Celsius. The required amount of buffer for each day was poured into a separate beaker and 1M $MgSO_4.7H_20$ and 1M $CaCl_2.2H_20$ were added to produce a 1:1000 and 1:500 dilution (1mM and 2mM) respectively. Three millilitres of buffer solution were added to three dishes labelled “transit”, “loading”, and “deesterification”. As stated earlier the “loading” dish also had 30uL of the dye solution added to it such that the cells on the coverslip could be loaded with the calcium-dependent dye.

Each coverslip was incubated in Dulbecco’s medium at 37 degrees Celsius with a CO2 level of 5%. When the coverslips were present in the loading or de-esterification dishes, the dishes were covered in foil to prevent photo-bleaching.

Calcium Imaging:

The epifluorescence calcium imaging experiments were performed on spinal and cortical astrocytes. Firstly, astrocytes were loaded with 1µM of the Ca^{2+} indicator fluo-5F AM (Invitrogen, Paisley, UK) in standard buffer solution for 30 minutes. Secondly, after the cells had been loaded with the calcium indicator dye for 30 minutes, the astrocytes were then

left for a further 30 minutes in a different dish, containing only 3ml of standard buffer solution, to de-esterify the accumulated fluo-5F AM.

After the astrocytes had completed their de-esterification process they were then placed into a two-component chamber; the first component, which housed the coverslip, was a grooved, plastic base which had been coated with silicon grease, and the second component was a stainless steel cylinder which was placed on top of the mounted coverslip to produce a watertight seal.

The imaging chamber was then transferred to the stage of an SP-98-FL inverted fluorescent microscope (Brunel Microscopes Ltd, Chippenham, UK) which used a 10x, 0.25 NA objective. The loaded astrocytes were excited at a wavelength of 480nm and a light intensity of 9%, both of which were controlled using a CoolLED pE-100 LED illumination system (CoolLED Ltd, Andover, UK) that delivered light directly to the microscope. The astrocytes were imaged at a frame rate of 1Hz for 1200 seconds with an exposure time of 100ms and 4x4 binning dimensions. The fluorescence emission (~520nm) was detected using an ORCA-ER C4742-95 camera (Hamamatsu Photonics Ltd, Welwyn Garden City, UK) and the camera and shutter were controlled using Micro-Manager 1.4 software. The field of view used in the images produced from the live calcium imaging was $7.82x10^{-4}$µm by $5.96x10^{-4}$µm.

Pasteur pipettes were used to manually displace bath solution with an excess (~2.5ml) of either buffer solution alone or buffer containing

stimuli in the absence or presence of [D-Ala2, N-MePhe4, Gly-ol]-enkephalin (DAMGO) at the indicated concentrations.

Spinal Astrocytes (Stimulus-alone Tests):

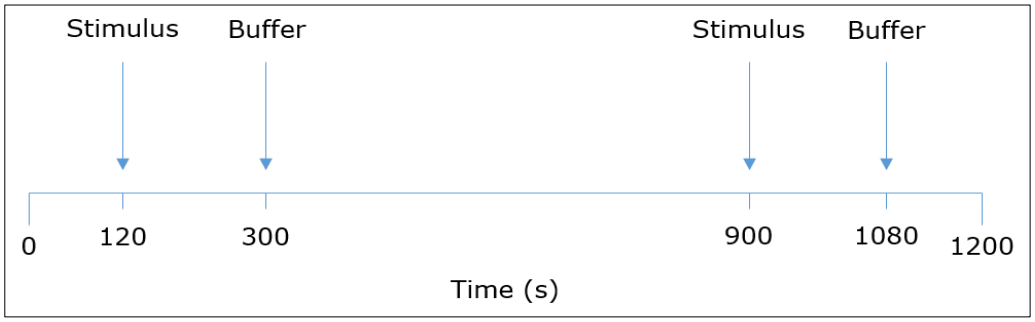

Figure 2: A timeline of how neonatal astrocytes were exposed to stimulation during live calcium imaging. The time course is displayed in seconds.

Neonatal spinal astrocytes were imaged using Micro-Manager 1.4 for 1200 seconds as shown in Figure 2. Initially, these cells were bathed in a buffer solution for 120 seconds after which the buffer solution was displaced with ~2.5ml of a stimulus-containing buffer solution using a Pasteur pipette. The stimulus present in the buffer solution was either 1uM ATP or 100nM SP. The astrocytes were bathed in the stimulus solution for a further 180 seconds, after which the solution was displaced by 2.5ml of standard buffer solution. The cells were then allowed to bathe in the buffer solution for a further 10 minutes after which a second application of the stimulus solution was administered via the displacement method used previously. After a further 180 seconds, the stimulus solution was displaced with standard buffer solution after which the astrocytes bathed for a further 120 seconds until the imaging process had finished.

Spinal astrocytes (Stimulus with DAMGO):

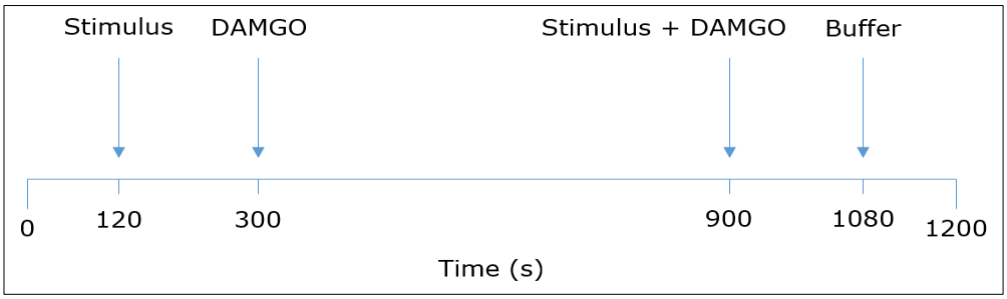

Figure 3: A timeline of how neonatal astrocytes were exposed to stimulation in the absence and presence of DAMGO during live calcium imaging. The time course is displayed in seconds.

Spinal astrocytes are initially bathed in a buffer solution for 120 seconds after which they are administered with a stimulus solution containing either 1uM ATP or 100nM via the displacement method. After a further 180 seconds the stimulus solution was displaced with a buffer solution containing 10uM DAMGO in which the cells are bathed for a further 10 minutes. After 900 seconds the DAMGO-containing buffer solution was displaced with a solution containing both 10uM DAMGO and a stimulus (100nM SP or 1uM ATP). The astrocytes are bathed in the DAMGO-stimulus mixed solution for a further 180 seconds after which the bath solution was displaced with standard buffer solution using a Pasteur pipette. The astrocytes were then bathed in the standard buffer solution for a further 120 seconds until the imaging process had been completed as also shown in Figure 2.

Cortical Astrocytes (ATP):

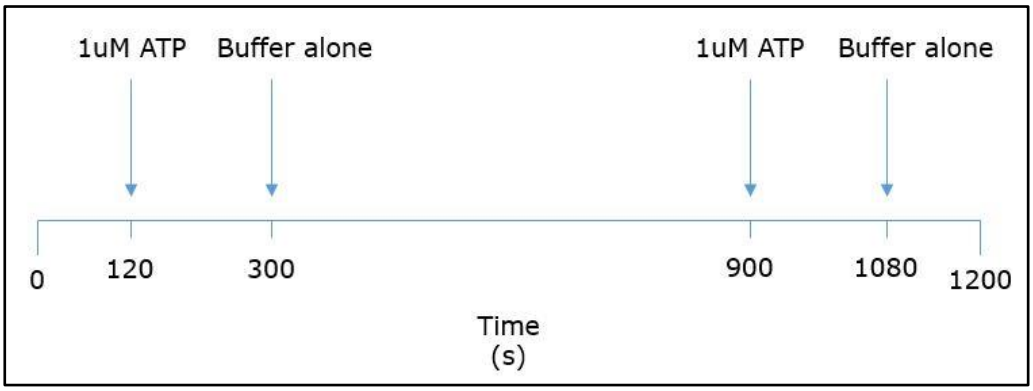

Figure 4: A timeline illustrating the time points at which cortical astrocytes were exposed to ATP or standard buffer solution. Time is displayed in seconds.

Cortical astrocytes that underwent calcium imaging with ATP as the chosen stimulus followed the same timing protocol as the spinal astrocytes. At 120 seconds, the cortical astrocytes were exposed to 1µM ATP in buffer via displacement of the previous bath solution. The cells remained in the ATP solution for a further three minutes, after which the ATP solution was displaced with ~2.5ml of standard buffer solution using a Pasteur pipette. The astrocytes were bathed in standard buffer solution for 10 minutes, after which the stimulation with ATP was repeated (at 900 seconds). At 1080 seconds, the ATP solution in which the astrocytes had bathed for three minutes, was displaced with standard buffer solution in which the cells bathed for the final two minutes of the imaging process.

Cortical Astrocytes (SP):

In light of the results of the spinal cord tests, the protocol was changed here such that calcium imaging tests involving SP were to proceed in the following manner. Firstly, tests in which substance P alone was used, followed the normal protocol as used in the ATP-alone and

SP-alone tests performed on spinal astrocytes. However, SP-with-DAMGO tests were performed by firstly, bathing the astrocytes in a buffer solution containing 10uM DAMGO for ten minutes and then measuring the initial response to a combined stimulus (100nM SP and 10uM DAMGO) after 600 seconds. After 780 seconds the bath solution was displaced manually with standard buffer solution in which the cells bathed for the remaining two minutes of the imaging process. Responses to 100nM SP were measured in the same manner as those treated with both SP and DAMGO i.e. they were bathed in buffer solution for an initial 600 seconds followed by treatment with 100nM SP via the displacement method.

Cortical Astrocytes (ATP with DAMGO):

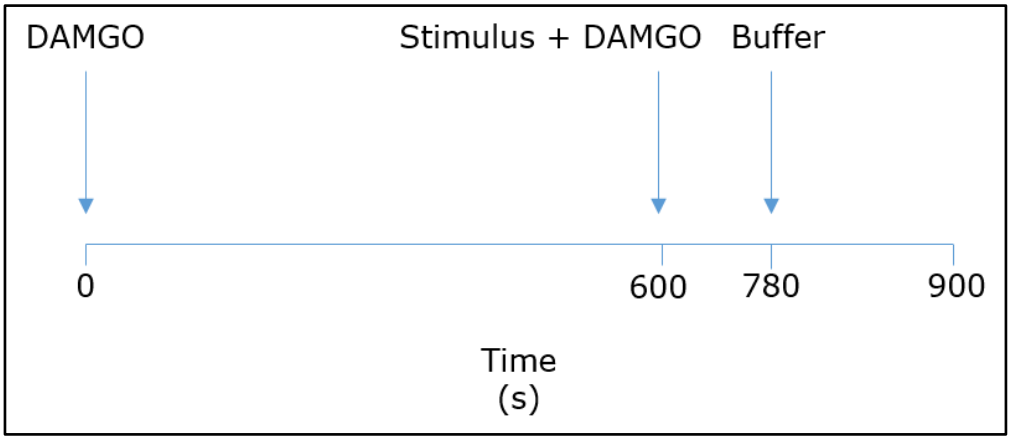

Figure 5: A timeline showing how cortical astrocytes were bathed in 10μM DAMGO for an initial 600 seconds prior to being treated with a buffer solution containing either 100nM SP or 1μM ATP in the presence of 10μM DAMGO for a further 180 seconds. The time course for the live calcium imaging is displayed in seconds.

In the experiments which looked at the effect of DAMGO on ATP-induced responses in cortical astrocytes (Figure 5), the cells were firstly pre-incubated with 10μM DAMGO for ten minutes. After ten minutes of

pre-incubation with DAMGO, the astrocytes were exposed to 1µM ATP and 10µM DAMGO in buffer via the displacement of the previous bath solution. The buffer solution containing ATP and DAMGO was replaced with a standard buffer solution at 780 seconds and the astrocytes were bathed in the buffer solution for the remainder of the time course. The results produced by the stimulation of astrocytes with ATP in the presence of DAMGO were compared to the initial responses of ATP-treated cortical astrocytes (120 – 300 seconds in Figure 4) to show whether pre-incubation with DAMGO had any impact on first-dose responses to ATP among astrocytes.

Cell fixing:

Cultured cortical astrocytes were divided into four groups: control, forskolin alone, DAMGO alone, and DAMGO with forskolin. The first (control) group had no additional solutions added to the culture media. The second group (forskolin alone) of astrocytes were incubated for three hours at 37°C (5% CO2) in media containing 100µM forskolin. The third group (DAMGO alone) were incubated for three hours at the same temperature and CO2 concentration as the second but with media containing 10µM DAMGO. The final group of astrocytes (DAMGO with forskolin) were incubated for three hours at 37°C (5% CO2¬) in media containing both 10µM DAMGO and 100µM forskolin.

After three hours of incubation, the media was removed via pipette and the cells were washed with phosphate buffer solution (PBS) at room temperature to ensure no material from the media was still in contact with the cells, and to reduce the likelihood of thermal shock when the

paraformaldehyde was added. After this, the PBS was removed via pipette and replaced with a 4% paraformaldehyde (PFA) solution, at approximately room temperature, in which the astrocytes were bathed for 10 minutes so that they became fixed. After this the fixative PFA solution was removed by pipette and replaced with a PBS solution for storage. The cells were stored at 4°C until they were required for the current study.

Bright-field imaging:

To assess the morphology of the cortical astrocytes, the coverslips were first mounted onto slides (Sigma-Aldrich, Gillingham, UK) using a single drop of Vectashield mounting solution (Vectashield, Peterborough, UK) and being placed carefully using fine forceps. The slides were then transferred to the stage of a Nikon Eclipse Ti microscope (Nikon UK Ltd, Surrey, UK). The cells were viewed using a 10x magnification (CFI60 objective) and a focus level of between 28500-3000µm which was when the cells had become visible on-screen. The images were taken with an Andor Zyla 4.2 sCMOS camera and shutter (Oxford Instruments PLC, Abington, UK) an exposure time of 100ms and a field of view size of 1.3312cm by 1.3312cm (2048px by 2048px). The camera and shutter were controlled using Micro-Manager 1.4 software.

Analysis:

Firstly, regions of interest were chosen whereby the each cell's nucleus were manually selected using the Time Series Analyzer v3.0 plugin (Department of Neurobiology, UCLA, USA) for ImageJ. The fluorescence intensity of each region of interest was given as the ratio of

the fluorescence at time t (after the background fluorescence had been subtracted) and the mean fluorescence of the cells immediately prior to the addition of the stimulus (F/F0). Analysis data was extracted using a script in MATLAB 2016.a. Cells which were defined as responsive to a stimulus (in other words, a cell that produces a calcium signal that reaches its nucleus) if the fluorescence of the cell increased by at least 1.045-fold (i.e. at least three standard deviations above the mean fluorescence intensity prior to stimulation). The peak amplitude is the maximum fold-change in fluorescence intensity (Fmax) for a given cell over the course of the imaging process. The number of spikes within a calcium response was also extracted from the time trace using the aforementioned MATLAB script.

Differences in the mean peak amplitude, number of calcium spikes, and percentage response (the percentage of all cells that were defined as responsive) among cells that were stimulated twice were compared statistically using a Wilcoxon matched-pairs signed ranks test. The peak amplitude, number of spikes, and responsiveness of cells subject to different conditions (i.e. on different coverslips) were measured using an unpaired Mann-Whitney test.

The stellation of cortical astrocytes used for bright-field imaging was assessed manually. Cells which exhibited condensed cell body, and narrowed and elongated processes that are characteristic of stellated cells were considered stellate. The phase contrast micrographs of glial cells before and after exposure to 100μM forskolin produced by Kempski et al in 1987 were used as a morphology guide (Kempski et al., 1987)

(Figure 6). The number of stellate cells in a field of view (1.3312cm by 1.3312cm) were counted and recorded as a percentage of the total number of cells. The mean percentage of stellate cells in each of the conditions previously outlined were compared using an unpaired Mann-Whitney test.

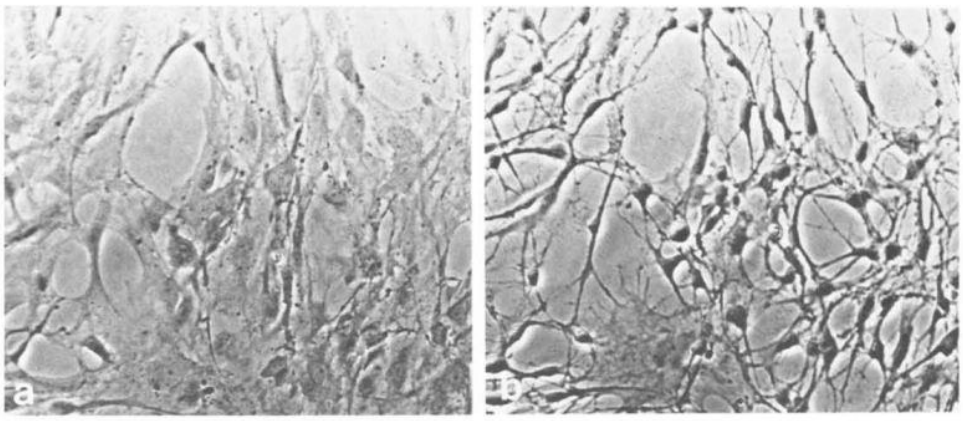

Figure 6: Phase contrast micrographs showing the changes in astrocyte morphology from non-stellate prior to forskolin treatment (left) to stellate following exposure to 100uM forskolin (right). These micrographs illustrate how the processes of the astrocytes constrict following forskolin exposure producing the stellate phenotype. (Kempski et al., 1987)

All statistical analyses were performed using GraphPad Prism 7.02 (GraphPad Software, La Jolla, CA, USA).

Results:

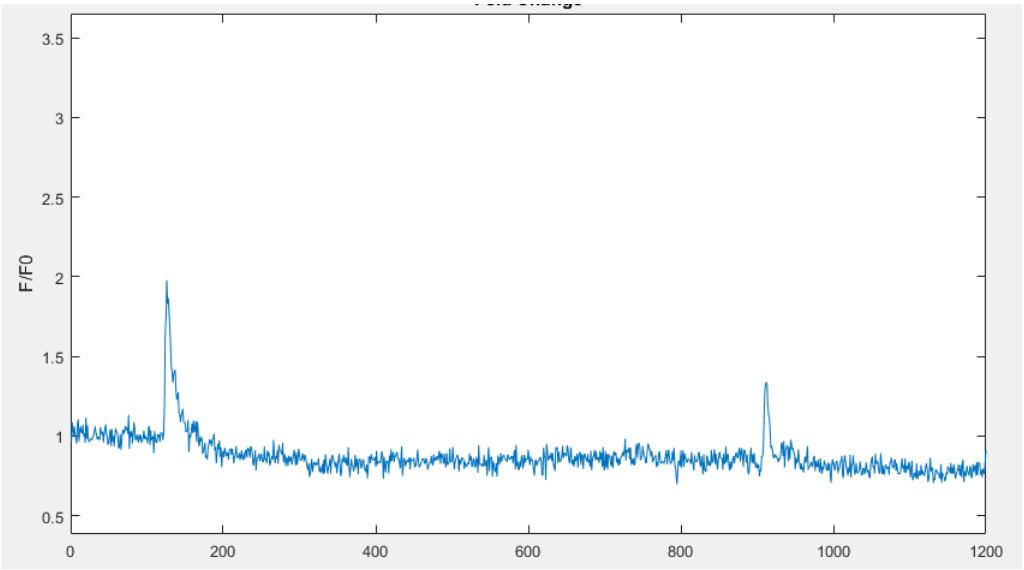

Figure 7: Typical time trace for ATP responses. Time is displayed in seconds and F/F0 is the fold change in fluorescence intensity.

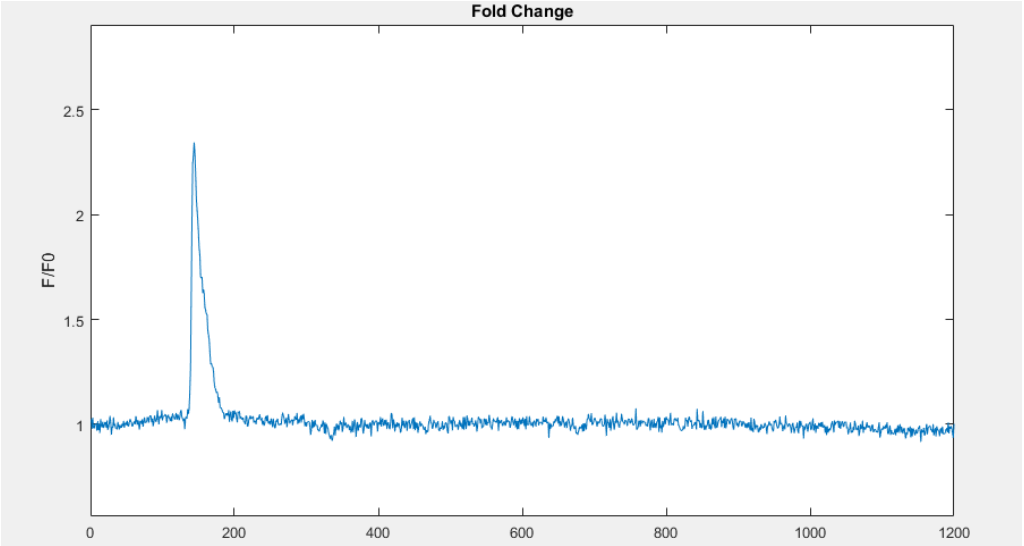

Figure 8: Typical time trace for SP responses. Time is displayed in seconds and F/F0 is the fold change in fluorescence intensity.

The effect of DAMGO on ATP responses in spinal astrocytes:

Here, the peak amplitude (Fmax/F0) of calcium responses elicited by spinal astrocytes in response to 1uM ATP stimulation in the absence and presence of 10uM DAMGO was measured using a MATLAB script

and analysed using paired Wilcoxon tests. The number of calcium spikes per response were also measured and analysed using the same means, however, the percentage of responding cells was analysed using a Fisher's exact test.

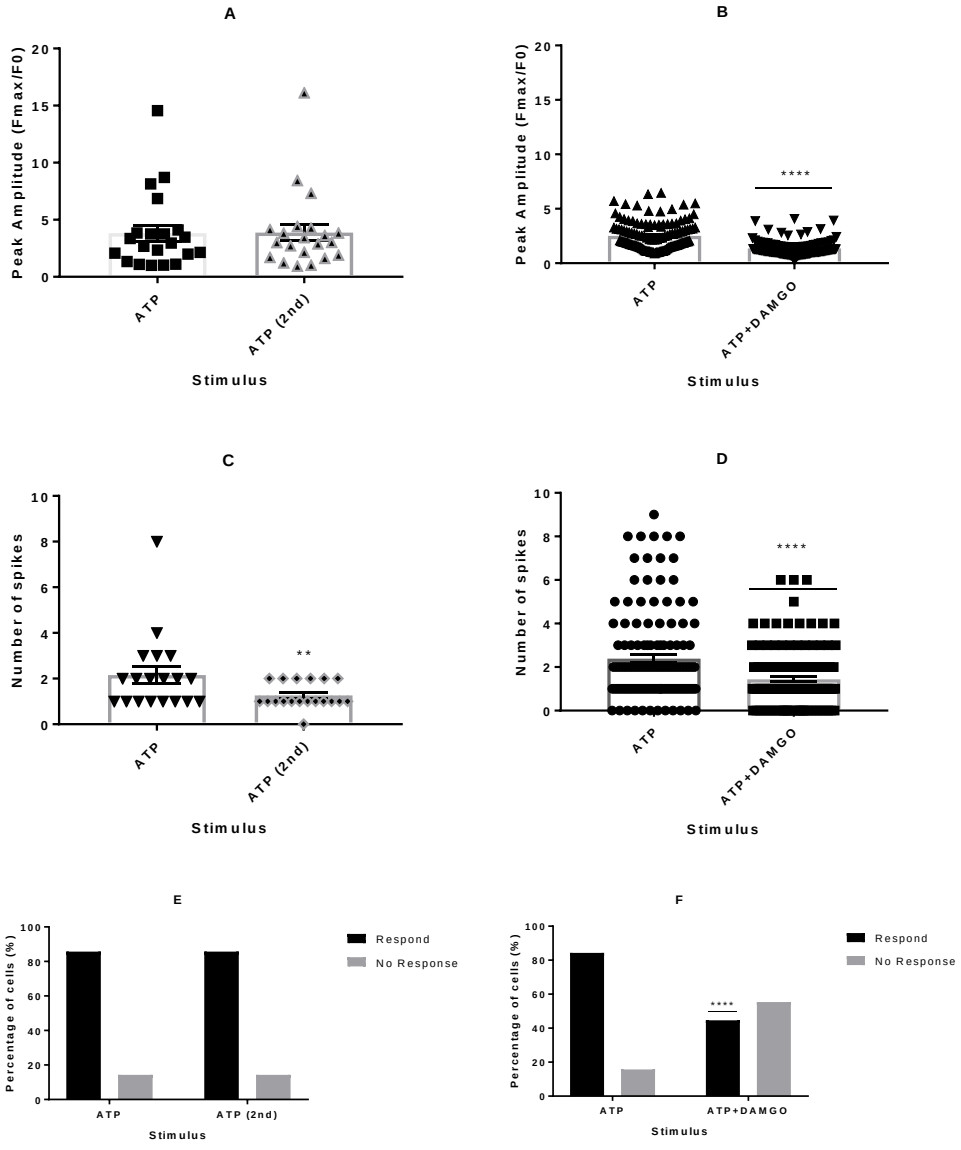

Figure 9: The mean peak amplitude of calcium responses (fluorescence intensity) among spinal astrocytes that had been stimulated with 1uM ATP twice (n=21 cells) [A] and those that had been stimulated with 1uM ATP and then 1uM ATP in the presence of 10uM DAMGO after a 10 minute wash period in which the cells were bathed in standard buffer solution (n=127 cells) [B]. The number of calcium spikes elicited by

cells responding to stimulation with 1uM ATP (once at 120 frames and once at 900 frames) (n=19 out of 21 cells) [C] and those responding to stimulation firstly with 1uM ATP and then 1uM ATP in the presence of 10uM DAMGO (n=116 out of 127 cells) [D]. The percentage of cells responding to stimulation with 1uM ATP twice [E] or 1uM ATP in both the absence and the presence of 10uM DAMGO [F]. Error bars are the mean ± SEM. Degrees of significance are calculated using paired Wilcoxon tests (A-D) and Fisher's exact tests (E-F) and are represented as p<0.05 (*) and p<0.0001 (****).

The peak amplitude of calcium responses elicited by spinal astrocytes, i.e. their maximum fluorescence intensity, in response to stimulation with 1uM ATP did not change significantly between the responses to the first treatment and the second treatment following a 10-minute wash period ($p>0.9999$); therefore, it can be stated that for spinal astrocytes repeated applications of ATP alone do not affect the magnitude of calcium responses (Figure 9A). However, reapplication of ATP in the presence of 10uM DAMGO significantly decreased the maximum amplitude of calcium responses among spinal astrocytes ($p<0.0001$) (Figure 9B). Regarding the number of calcium spikes, a second stimulation with 1uM ATP after a 10-minute wash period did trigger a significant reduction in the number of calcium spikes ($p=0.0371$) (Figure 9C), however, a second stimulation with 1uM ATP in the presence of 10uM DAMGO (Figure 9D) also caused a significant reduction in calcium spike number ($p<0.0001$). An unpaired Mann-Whitney test was used to compare the number of calcium spikes produced in response to the second application of ATP in the presence and absence of DAMGO. It showed that the difference between the numbers of evoked calcium spikes were not significantly different from

each other ($p = 0.8431$). Due to the much lower probability that the results were due to chance among those treated with both ATP and DAMGO compared to those that only had a second stimulation with ATP, it can be deduced that DAMGO has a significant effect on calcium spike number. The Fisher's exact test revealed that a second stimulation with 1uM ATP alone (Figure 9E) does not elicit a lower percentage of cells responding to stimulation whereas a second stimulation with ATP in the presence of DAMGO does cause a significant decrease in the response rate of spinal astrocytes ($p<0.0001$) (Figure 9F).

The effect of DAMGO on SP responses in spinal astrocytes:

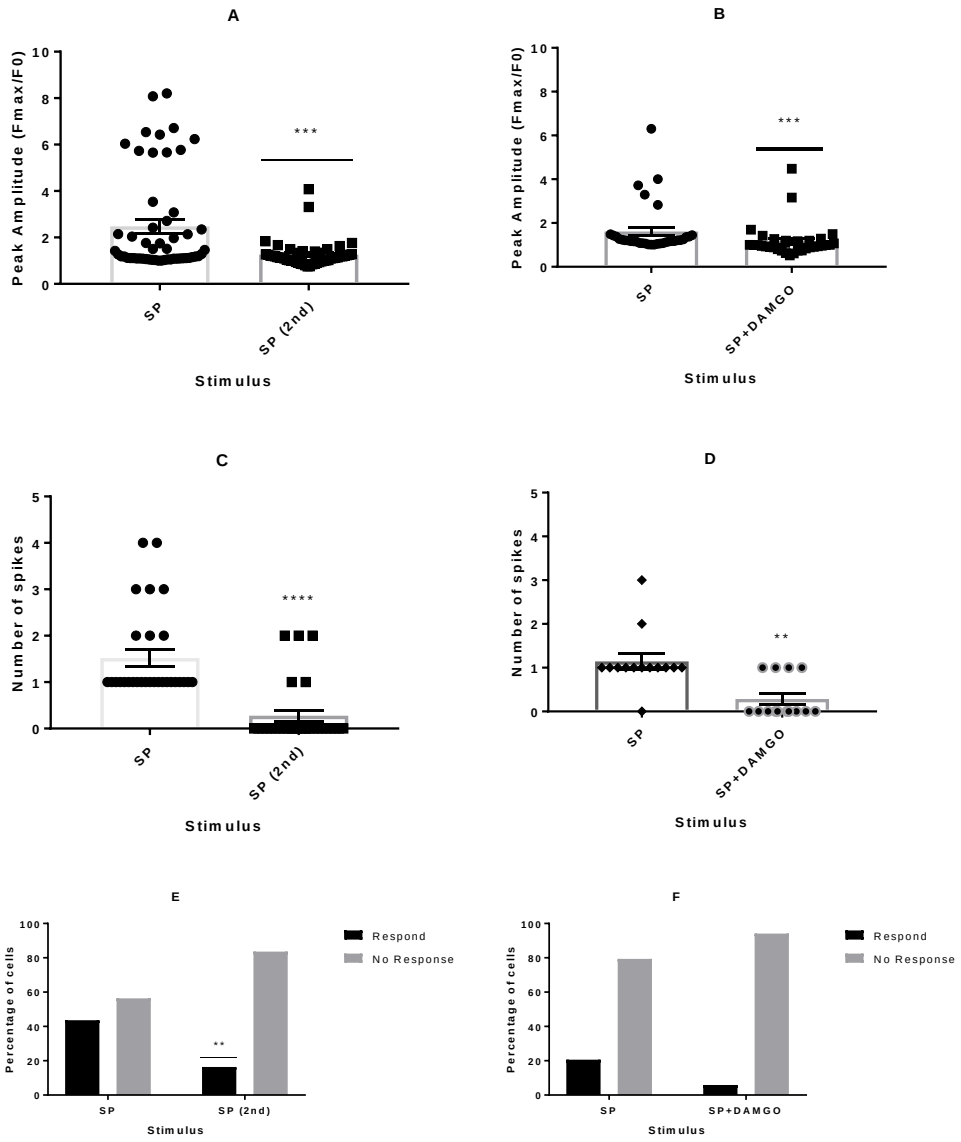

Figure 10: The peak amplitude of calcium responses elicited by spinal astrocytes following stimulation with SP alone twice (n=53 cells) (A) and with SP in the absence and presence of 10uM DAMGO (n=32 cells) (B). (C-D) The number of calcium spikes per response elicited by spinal astrocytes that had been stimulated with 100nM SP alone twice (n=26 out of 53 cells) after a 10 minute wash period or had been stimulated with SP in the absence and presence of DAMGO (n=14 out of 32 cells). (E-F) The percentage of cells responding to stimulation with two doses of 100nM SP alone (n=53 cells) and that of those cells responding to SP in the absence and

presence of DAMGO (n=32 cells). Error bars represent the mean ± SEM and statistical significance was calculated using paired Wilcoxon tests (A-D) and Fisher's exact test (E-F). p<0.01 (**), p<0.001 (***), and p<0.0001 (****).

The peak amplitudes of calcium responses elicited by spinal astrocytes, according to paired Wilcoxon tests, in response to SP stimulation are significantly reduced by both a second stimulation with 100nM SP and a second stimulation with 100nM SP in the presence of 10uM DAMGO (p=0.0005 and p=0.0002 respectively) (Figures 10A and 10B). The number of calcium spikes per calcium response elicited by responding cells was both significantly affected by a second stimulation with 100nM SP alone (p<0.0001) and, according to Figure 10D, by a second stimulation with 100nM SP in the presence of 10uM DAMGO (p=0.0054). However, an unpaired Mann-Whitney test comparing the number of calcium spikes produced by those treated with only a second dose of SP and those treated with a second dose of SP in the presence of DAMGO showed that there was no significant difference between those groups (p=0.6724) i.e. any difference between them is approximately 67% due to random chance. Similarly, the percentage rate of responding cells is significantly reduced following a second stimulation with 100nM SP alone (a decrease from 43.64% to 16.36%) (Figure 10E; p=0.0032) whereas it is not affected by stimulation with both SP and DAMGO (20.59% response rate vs 5.88% response rate) (p=0.1497).

The effect of DAMGO on ATP responses in cortical astrocytes:

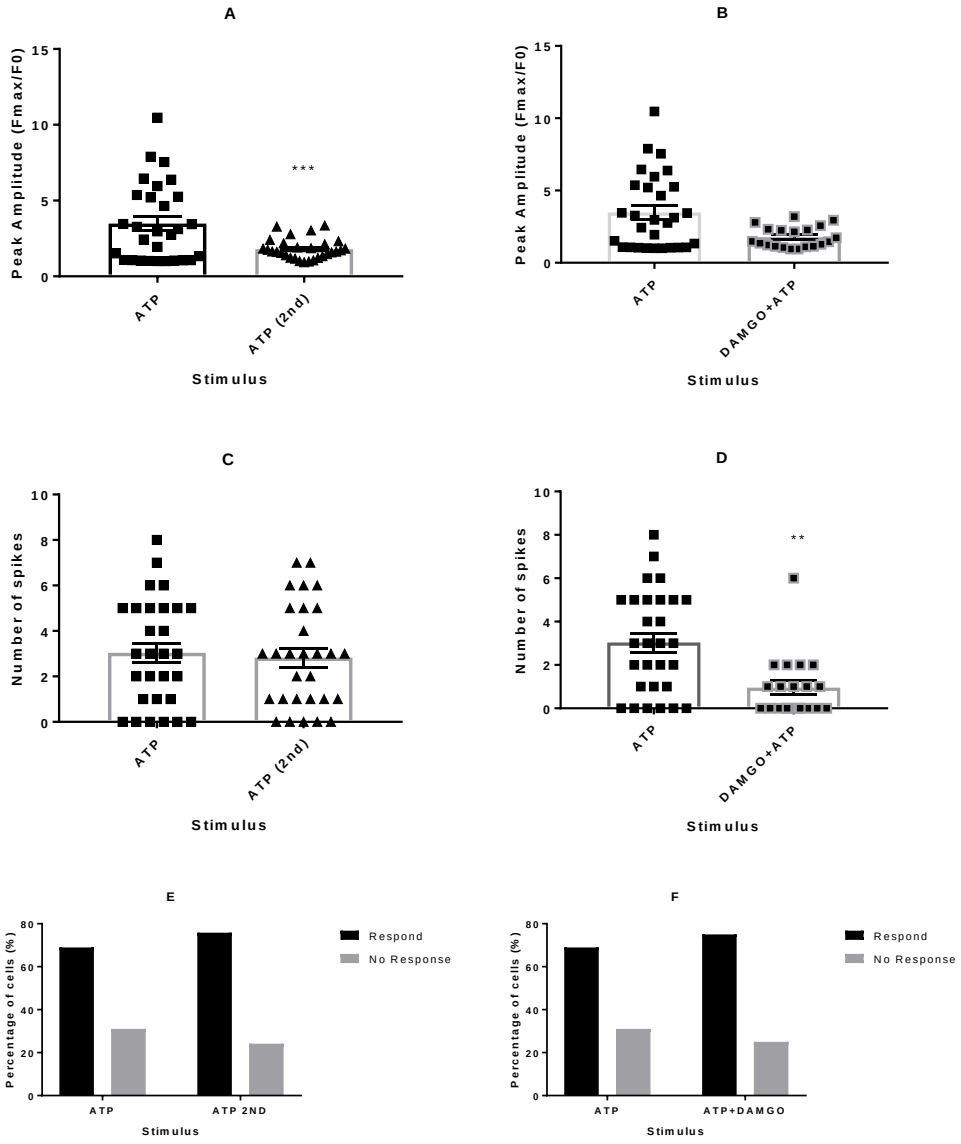

Figure 11: The peak amplitude (Fmax/F0) of calcium responses elicited by cortical astrocytes in response to 1uM ATP followed by (A) a second dose of 1uM ATP in buffer (n=29 cells) after a 10-minute wash period and (B) 1uM ATP and 10uM DAMGO in buffer (n=20 cells) after a 10-minute wash period. (C-D) The number of calcium spikes per calcium response elicited by cortical astrocytes following stimulation with 1uM ATP compared to (C) those elicited after a second dose of 1uM ATP and (D) 1uM ATP and 10uM DAMGO in buffer after a 10-minute wash period. (E-F) The percentage of cells which responded to stimulation with 1uM ATP compared to [E] the percentage responding after a second dose of 1uM ATP in buffer after a 10-

minute wash period and to [F] the percentage of cells that responded to stimulation with both 1uM ATP and 10uM DAMGO. Error bars represent the mean ± SEM and degrees of significance were calculated using paired Wilcoxon tests (A and C), unpaired Mann-Whitney tests (B and D), and Fisher's exact test (E and F). p<0.01 (**) and p<0.001(***).

The peak amplitude of calcium responses elicited by cortical astrocytes in response to 1uM ATP was significantly reduced upon re-stimulation with 1uM ATP after a 10-minute wash period (Figure 11A; p=0.0004 (Wilcoxon test)), however, unlike spinal astrocytes that were stimulated with both 1uM ATP and 10uM DAMGO, DAMGO does not significantly affect the peak amplitude of calcium responses (Figure 11B; p=0.0567 (Mann-Whitney)). For the number of calcium spikes produced in each calcium response, however, the converse is true whereby a second stimulation with 1uM ATP in buffer does not significantly affect the number of calcium spikes (mean= 3.034 and 2.828 spikes respectively; p=0.6598), yet the number of spikes produced by cells treated with 1uM ATP and by cells treated with both 1uM ATP and 10uM DAMGO were significantly different according to the Mann-Whitney test (Figure 11D; p=0.0012). According to the Fisher's exact tests, neither a secondary stimulation with 1uM ATP (Figure 11E) nor stimulation with 1uM ATP in the presence of 10uM DAMGO significantly affected the percentage of cells which responded to ATP stimulation (p=0.7696 and p=0.7536 respectively).

The effect of DAMGO on SP responses in cortical astrocytes:

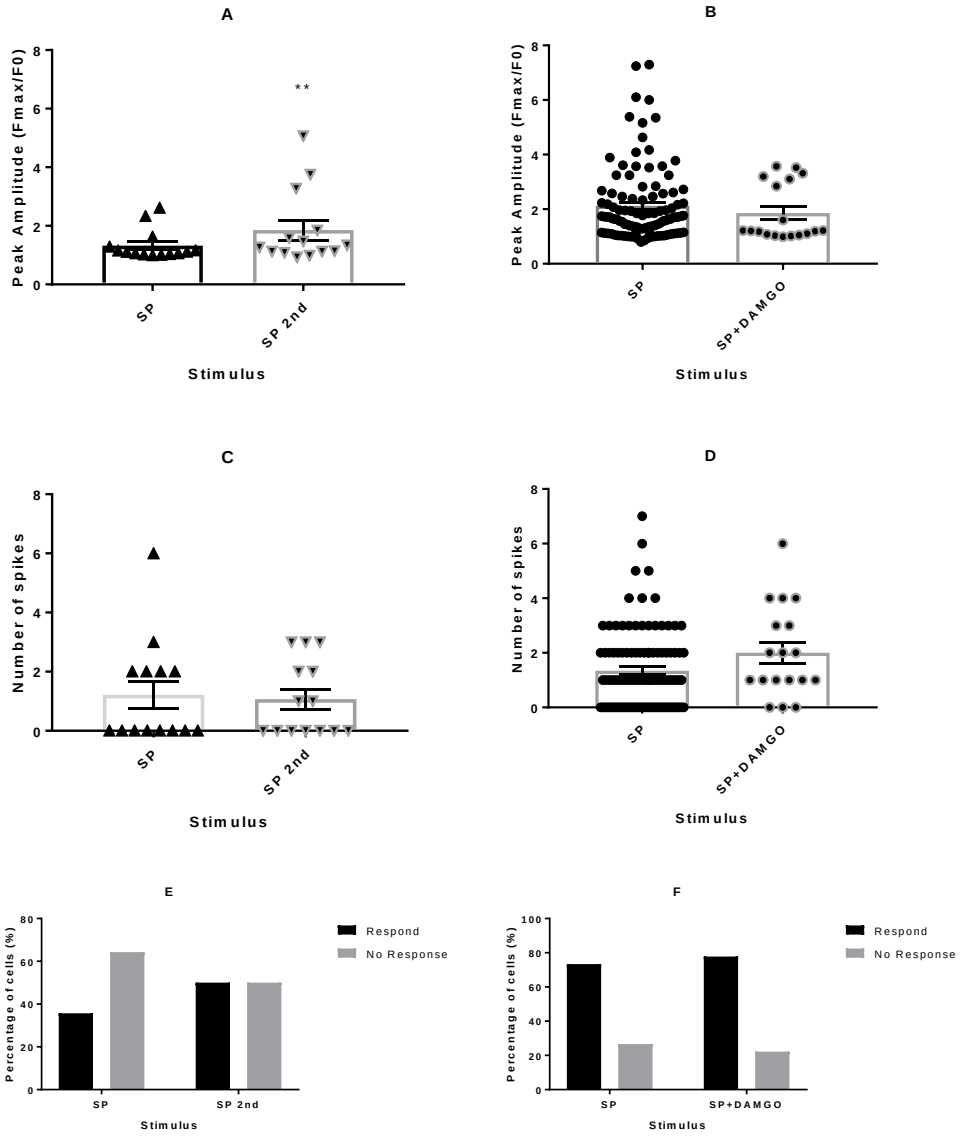

Figure 12: The peak amplitude of calcium responses (Fmax/F0) in response to stimulation with 100nM SP compared to a second stimulation with 100nM SP in buffer after a 10-minute wash period (n=14 cells) (A). (B) The peak amplitude of calcium responses elicited by all cortical astrocytes that were stimulated with 100nM SP (n=106 cells) compared to the mean peak amplitude of calcium responses elicited by cells treated with both 100nM SP and 10uM DAMGO after being incubated with 10uM DAMGO for 10 minutes (n=18 cells). (C) A comparison of the number of calcium spikes in each calcium response following an initial and a secondary dose of 100nM

SP. (D) The average number of spikes produced by cortical astrocytes following an initial exposure to 100nM SP compared to the number produced by astrocytes that were exposed to both 100nM SP and 10uM DAMGO after being pre-incubated with 10uM DAMGO for 10 minutes. (E-F) The percentage of cells that responded and did not respond to either an initial dose of 100nM SP or a second dose of 100nM SP (E) or to stimulation with 100nM SP in the presence of 10uM DAMGO (F). Error bars represent the mean ± SEM. Degrees of significance were calculated using Wilcoxon tests (A and C), Mann-Whitney tests (B and D), and Fisher's exact tests (E and F).

Figures 12A and 12B show that a secondary exposure to 100nM SP significantly increases the peak amplitude of calcium responses ($p=0.0031$) according to a paired Wilcoxon test and that initial responses to 100nM in the presence of 10uM DAMGO following pre-incubation with 10uM DAMGO for 10 minutes are not significantly different to the average peak amplitude of calcium responses elicited by cortical astrocytes solely exposed to 100nM SP ($p=0.2725$). Neither the number of spikes produced by cortical astrocytes exposed to a second dose of 100nM SP (mean = 1.071 spikes) nor those produced by astrocytes that respond to 100nM SP in the presence of 10uM DAMGO were significantly different from the average number of spikes per response produced by astrocytes exposed to an initial dose of 100nM SP ($p=0.9766$ and $p=0.0897$ respectively). Cortical astrocytes show no significant change in responsiveness following a second dose of 100nM SP (Figure 12E; $p=0.7036$; 35.714% initial responsiveness and 50% after the second dose). Cortical astrocytes exposed to 100nM SP and 10uM DAMGO simultaneously do not show any significant difference in responsiveness compared to the average responsiveness of all cortical astrocytes which

had an initial dose of 100nM SP (Figure 12F; 73.404% SP-alone vs 77.78% SP with DAMGO; p=0.7036 and p>0.9999 respectively). There was a significant difference in the initial response rate to SP among those that were treated with SP twice (Figure 12E) and the initial responses to SP by cortical astrocytes in general (Figure 12F) which were compared to the initial responses to SP in the presence of DAMGO (p = 0.0105). The possible reasons for this disparity, however, will be discussed in the later sections of this thesis.

The effect of DAMGO on astrocyte stellation:

Here, the change in astrocyte morphology in particular, the degree to which the cultured astrocytes exhibit a stellated (star-like) phenotype as opposed to their default flat phenotype after three hours of incubation either under control conditions, in the presence of 10µM DAMGO, 100µM forskolin, or both 10µM DAMGO and 100µM forskolin was measured. This was done by manually counting the cells within the field of view that expressed a stellate morphology and expressing that as a percentage of the total number of cells in that field of view.

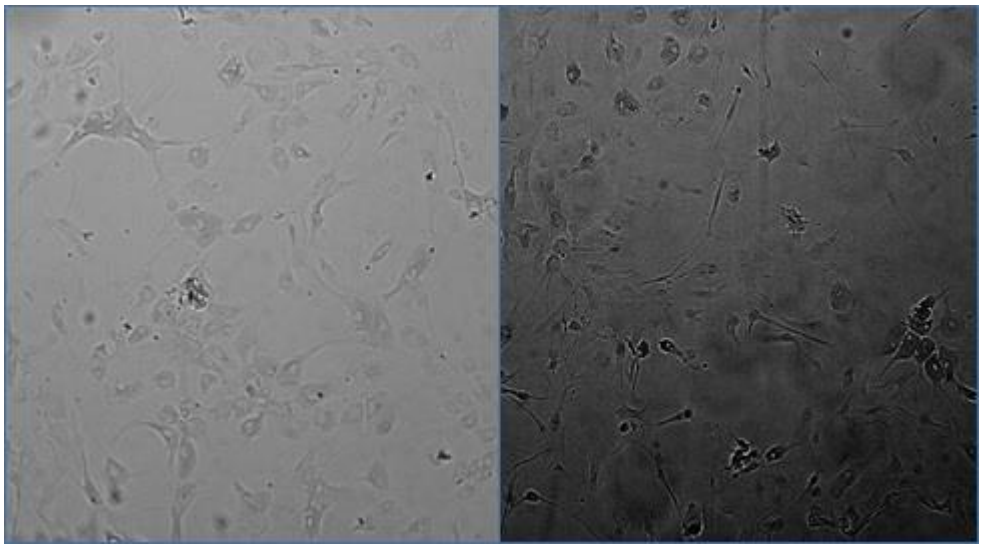

Figure 13: Bright-field micrographs (10x magnification) of cultured cortical astrocytes after being fixed with 4% PFA solution after being incubated for three hours at 37°C under control conditions (left) or in the presence of 100μM forskolin (right).

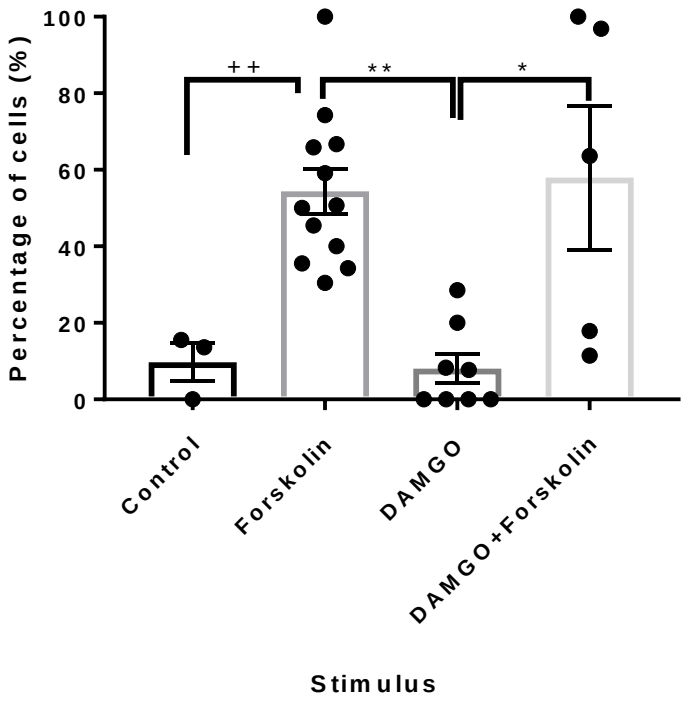

Figure 14: The percentage of cortical astrocytes that express a stellate morphology after three hours of incubation and being fixed using a 4% PFA solution. The treatment groups (the control group – 94 cells, 3 regions of interest; those that had been incubated in 100µM forskolin – 423 cells, 12 regions of interest; those that had been incubated with 10µM DAMGO – 110 cells, 8 regions of interest; and those that had been incubated in a solution containing 100µM forskolin and 10µM DAMGO – 169 cells, 5 regions of interest) were compared against each other using both Kruskal-Wallis test and multiple Mann-Whitney tests. Degrees of significance are displayed as p<0.05 (*) and p<0.01 (**) for the Kruskal-Wallis test and as p<0.01 (++) for the Mann-Whitney test. Error bars represent the mean ± SEM.

The median percentage stellation among cortical astrocytes vary among the treatment groups in general according to the Kruskal-Wallis test (p = 0.0007). However, both cortical astrocytes incubated with solely DAMGO and those that were incubated with DAMGO in the presence of forskolin did not vary significantly in their stellation prevalence compared to the control group (p>0.9999 and p = 0.3209 respectively). The

DAMGO-treated astrocytes did exhibit stellate morphologies at a significantly lesser rate than those treated with forskolin alone and those treated with DAMGO in the presence of forskolin ($p = 0.0015$ and $p = 0.0409$ respectively). The Kruskal-Wallis tests show that the control group was not significantly different compared to the forskolin-treated group ($p = 0.1026$), however, a Mann-Whitney test was also performed to compare the treatment groups and the Mann-Whitney test stated that the control and forskolin-treated groups did vary significantly ($p = 0.0044$). Given that the DAMGO and control groups are not significantly different from each other, it is most likely that the control group and forskolin-treated group are indeed significantly different from each other and that the disparity between the test results are a function of low sample numbers.

Discussion:

Regional differences in astrocytic responses to ATP:

The responsiveness and peak amplitude of calcium responses elicited by spinal astrocytes are significantly reduced in the presence of DAMGO, however, a comparison between the numbers of calcium spikes produced upon a secondary stimulation of solely ATP (Figure 9C) and with ATP in the presence of DAMGO (Figure 9D) showed that although the number of spikes elicited was significantly reduced from those produced after the initial stimulation in both cases, there was no statistically significant difference between them. Among cortical astrocytes, however, the second application of ATP alone caused a significant decline in the peak amplitude of calcium responses. Regarding initial responses to ATP alone, there was no significant difference in the peak amplitudes of calcium responses among spinal and cortical astrocytes according to a Mann-Whitney test ($p = 0.5014$). However, the amplitudes of calcium responses following both a secondary application of ATP alone and of ATP and DAMGO, there are significant differences between those produced by spinal and cortical astrocytes ($p = 0.0009$ and $p = 0.0091$ respectively). This suggests that there may be a degree of regional heterogeneity in regards to how the P2Y1 receptors, and other ATP-binding receptors, function, and in how mu-opioid receptors operate, like how there is astrocytic heterogeneity in their expression of GFAP and IL-6 (Yoon et al., 2017). The presence of DAMGO also appears to only significantly reduce the response rate of

spinal astrocytes to ATP (Figure 9F) whereas the percentage of cortical cells responding to ATP was not affected by DAMGO (Figure 11F).

Astrocytic responses to Substance P:

Among spinal astrocytes, it is clear that the peak amplitude of calcium responses (Figure 10 A-B), the number of calcium spikes produced (Figure 10 C-D), and the percentage response rate (Figure 10 E-F) are reduced in response to a secondary application of SP in both the presence and absence of DAMGO. However, these reduced responses are not statistically different from one another meaning that either DAMGO has no real effect on responsiveness to SP or that the effect of DAMGO is masked by an effect which occurs following the first application of SP. The latter of which would explain why only a single peak is present in Figure 8.

Adult human astrocytes were shown to express neurokinin-1 receptor isoforms and to functionally respond to SP exposure (Burmeister et al., 2017). Receptors which bind SP on the membranes of the spinal neurons of adult male Sprague-Dawley rats undergo endocytosis (Honoré et al., 1999), and this neurokinin-1 receptor internalisation is inhibited by intrathecal injections of 20ug of morphine (Takasusuki and Yaksh, 2011). From the results of the current study, it could be suggested that perhaps the significant inhibition of calcium responses seen among spinal astrocytes following their initial exposure to SP (Figure 10) provides indirect evidence of neurokinin-1 receptors on the surface of the astrocytes indeed undergoing internalisation, however,

this was not measured in the current study and, therefore it cannot be said with certainty that this what causes this effect.

Among cortical astrocytes, however, Figures 12B and 12D suggest that pre-incubation with DAMGO neither significantly reduces the peak amplitude of calcium responses nor the number of spikes elicited during release. However, an issue with the current study's findings is that the number of coverslips which were used to analyse the effects of SP in the presence of DAMGO among cortical astrocytes was relatively small meaning that the true effect size of DAMGO may be obscured and that it could produce significant inhibition amongst a large enough sample.

Differences between ATP-induced and SP-induced responses:

The results of the current study have shown that neonatal astrocytes, in regard to their ATP signalling, are affected by DAMGO in an inhibitory manner. Among both spinal and cortical astrocytes, the peak amplitude of ATP-evoked calcium responses are reduced in the presence of DAMGO, though only significantly among spinal astrocytes. This effect could be due to a decrease in the sensitivity of the P2Y1 receptor which binds extracellular ATP resulting from the binding of DAMGO, a mu-opioid receptor agonist, to its receptor. However, this is most likely due to the positive feedback loop housed within astrocytes as exposure to extracellular ATP induces further ATP release from astrocytes as a means of inducing calcium waves in neighbouring

astrocytes and propagating signals to carry information to what would be other parts of the central nervous system *in vivo* (Troadec et al., 1999; Anderson et al., 2004). As previously mentioned, this increase in the responsiveness of astrocytes within any given field of view which is most likely due to intracellular ATP synergistically triggering calcium activity in neighbouring cells alongside the binding of extracellular ATP to P2Y1 receptors expressed by those astrocytes that, had their intracellular concentration of ATP progressively increase leading to basal ATP levels being closer to the threshold at which calcium waves would be evoked (Troadec et al., 1999; Anderson et al., 2004). This autocrine signalling is not induced by the binding of extracellular SP to neurokinin-1 receptors on the membrane surface, therefore, the average number of calcium bursts released from astrocytes treated with SP (Figures 10C-D and 12C-D) is not increased by increased basal concentrations of calcium-wave inducing stimuli like how the average is increased among those astrocytes that were treated with ATP.

The pre-incubation of cortical astrocytes with DAMGO prior to SP application does not significantly reduce the number of calcium spikes produced compared to those treated with SP alone (Figure 12D). Similarly, among spinal astrocytes, those that were treated with a secondary application of SP alone and those that there were treated with a combined stimulus of SP and DAMGO did not differ significantly in regards to the number of calcium spikes evoked following stimulation (Figure 10C-D). Therefore, among spinal astrocytes, it could be argued that the small difference between the mean peak amplitudes of those

treated with a second dose of SP alone and those treated with SP in the presence of DAMGO is due, in part, to the internalisation of neurokinin-1 receptors on the astrocytic membrane (Honoré et al., 1999) and a possible decrease in the sensitivity of neurokinin-1 receptors that were not previously bound with SP.

Stellation:

Astrocytes undergo a morphological change from a characteristic flat shape to one from which narrow processes extend outwards, producing a fibrous star-like shape in response to multiple forms of chemical stimulation. This process is called stellation. One example of a stellation-inducing factor is extracellular ATP which when in high micromolar to low millimolar concentrations reproduces many features that are associated with reactive gliosis (Neary et al., 1994). ATP is involved in the activation of astrocytes and can be released by previously activated microglia in response to CNS injury (Liu et al., 2011; Dou et al., 2012). Extracellular ATP induces stellation in cortical astroyctes by causing an increase in the intracellular concentration of cAMP triggered by P2Y1 receptors on astrocytic membranes binding ATP; though astrocytes in different brain regions undergo stellation to different degrees depending on the concentration of cAMP present (Won and Oh, 2000). Cerebellar astrocytes, for example, can be induced to undergo stellation at lower levels of 8-CPT-cAMP (a membrane-permeable analogue of cAMP), whereas to produce a maximal stellation effect in all brain regions apart from the hypothalamus a higher concentration of 250µM was needed according to Won and Oh's study.

The data presented in Figure 14 show that incubating neonatal cortical astrocytes with 100μM forskolin for three hours significantly increased the prevalence of stellate cells compared to astrocytes that were incubated under control conditions. There was a disparity in the significance between the median prevalence of stellate cells among forskolin-treated astrocytes and those in the control group according to the Kruskal-Wallis test and the Mann-Whitney test. The former deemed the difference to be statistically insignificant whereas the latter stated that the difference was significant. However, since the ability of forskolin to induce stellation, via increasing cAMP activity through adenylate cyclase activation (Totsuka et al., 1983), in astrocytes is well-established; and that forskolin has been compared to both AMP and 5-aminoimidazole-4-carboxamide-1-β-D-ribofuranoside (AICAR) (Favero and Mandell, 2007), the latter of which is sold under the commercial name *Acadesine* and is used in the treatment of acute lympoblastic leukaemia (Cronstein and Kamen, 2007), the result of the Mann-Whitney test is more likely to be correct and that the disparity between the statistical outcomes is probably a function of a low number of samples.

Incubation with 10μM DAMGO for three hours prior to fixation did not significantly impact the prevalence of stellate morphologies among the neonatal astrocytes compared to those in the control group. Nor did the presence of DAMGO significantly impact forskolin-induced stellation among cortical astrocytes. This is despite the opposite effects that DAMGO and forskolin have on cAMP activity in cells, where DAMGO decreases cAMP activity through the inhibition of adenylyl cyclase via a

G_o-dependent mechanism (Carter and Medzihradsky, 1993) and forskolin causes an increase in intracellular cAMP concentrations via the activation of adenylate cyclase as previously stated (Totsuka et al., 1983).

Studies that have used cell membranes from rat brains which were solubilised and treated with various concentrations of DAMGO for 10 minutes have shown that in adult rats 10uM DAMGO reduced forskolin-induced adenylyl cyclase activity by 54%, producing a net amount of cAMP weighing 3.28pmoles (Santhappan et al., 2015). However, Santhappan et al's work did not specify that this effect was solely in rat cortical astrocytes but rather from a mixture of cortical cell membranes. Therefore, later work could be done on astrocytes to observe whether this phenomenon is visible among astrocytes and more specifically among neonatal astrocytes.

In the experiments performed as part of the current study, DAMGO was applied 10 minutes prior to a three-hour incubation period with forskolin. Enzymatic degradation studies which examined DAMGO among other synthetic opioid receptor agonists showed that *in vivo* DAMGO has a half-life of 14.4 minutes (Szeto et al., 2001). However, due to the absence of many of the metabolic pathways that would be present in a living animal, among cultured astrocytes it is not known how the half-life of DAMGO would be affected. As a result, the data presented in Figure 14 show that chronic exposure to DAMGO, without reapplication, during forskolin treatment does not significantly inhibit the ability of forskolin to induce stellation in cortical astrocytes.

It should be noted that three-hour long pre-treatments of mouse HEK 293 cells with DAMGO resulted in a three-to-four fold compensatory increase in cAMP accumulation resulting from forskolin exposure (Blake et al., 1997). Blake et al's findings may provide a reason as to why despite the opposite effect on cAMP activity, the exposure of neonatal astrocytes to both DAMGO and forskolin for three hours did not cause any significant change in stellation rate, however, although the results of the current study show a similar effect, it cannot be said with certainty that the lack of significant difference between the stellation rates of the forskolin-alone group and the DAMGO-with-forskolin group is due to a compensatory increase in cAMP accumulation as this was not measured in the current study.

Future Implications:

Though some questions have been answered by the results of the current study, there are many questions that these results pose. Firstly, the mean peak amplitude of initial calcium responses does not vary significantly among spinal and cortical astrocytes when treated with the same stimulus. However, the peak amplitudes of initial responses do vary between stimuli though according to a Kruskal-Wallis test only among spinal astrocytes but due to the low sample size of cortical astrocytes treated with ATP compared to with SP, the reported insignificance of the difference may be inaccurate. The question that therefore arises would be what exactly causes the differences in the nature of calcium responses to each stimulus among neonatal astrocytes. As already suggested, one hypothesis for the greater size and number of calcium

responses among ATP-treated cells compared to SP-treated cells could be due to the synergism between initial binding of extracellular ATP and the ATP-induced autocrine release of ATP throughout the syncytium which, in turn, would increase baseline calcium levels within neighbouring cells so that they are consistently closer to the spike-emission threshold (Troadec et al., 1999; Anderson et al., 2004). The compounding of calcium release may also partly explain why the mean maximum fluorescence intensity (peak amplitude) produced by ATP-treated cells was generally higher than that of SP-treated cells in the current study.

Secondly, although it has been shown that astrocytes do indeed express neurokinin-1 receptors which internalise upon being bound to SP (Honoré et al., 1999; Burmeister et al., 2017), there is still some uncertainty as to the degree to which the mu-opioid receptor, and by extension the impact of DAMGO, is functionally coupled to the activity of neurokinin-1 receptors particularly in regard to those receptors that are concurrently internalised. However, it is known that opioid receptor activation can inhibit the release of SP from afferent neurons in neonatal rats (Thomson et al., 2008). Due to the intimate modulatory interactions that neurons and astrocytes have in the central nervous system, and that astrocytes in culture are reactive to SP as shown in the results of the current study, there could be reason to suggest that the same phenomenon occurs in astrocytes.

Opioid receptors and neurokinin-1 receptors are co-localised on cells in the central nervous system (Pinto et al., 2008), and studies have

shown that opioid receptor ligands can alter the manner in which, or the degree to which, neurokinin-1 receptors internalise once bound, however, in the spinal cord they do not alter the binding of SP to neurokinin-1 receptors (Trafton et al., 1999). Also in regard to receptor internalisation, the mu-opioid receptor to which morphine and DAMGO are highly-specific can also internalise, however, morphine is unable to induce and or promote the endocytosis of this receptor whereas DAMGO is able to potentiate the internalisation of mu-opioid receptors (Finn and Whistler, 2001). Therefore, the experiments performed using DAMGO in the current study should be repeated with other similarly potent mu-opioid receptor agonists such as morphine that do not possess the ability to promote internalisation in order to observe the effect, if one exists, that receptor endocytosis has on calcium signalling induced by either coupled receptors or by intracellular chemical messengers such as intracellular ATP or cAMP.

Since, the initial binding of SP causes neurokinin-1 receptor internalisation, it is difficult to assess whether DAMGO in neonatal astrocytes has a real effect on signalling as those cells were treated with DAMGO after their initial exposure to SP. A small sample size may have been an impediment to observing whether pre-incubation with DAMGO had any effect on initial SP responses; as such these tests should be repeated with a larger sample size in the future. To observe whether DAMGO has any impact on the rate of receptor internalisation, the tests performed in the current study should be done in a reverse manner i.e. the cells should be pre-treated with DAMGO, then exposed to SP in the

presence of DAMGO followed by a secondary application of SP. Comparing the degree of calcium response size reduction would allow one to determine the effect of pre-activation of mu-opioid receptors.

Throughout the duration of the current study, there was some periods in which the pH of the working buffer solution was not effectively calibrated, initially due to a lack of NaOH but also due to unforeseen hardware issues which were later resolved. The subtle variations in pH may have had some effect on the responses elicited by astrocytes and this may have had some regional dependence i.e. a more pronounced effect in either the cortical or spinal regions. To combat this in future work, the pH of not just the working buffer but also the solutions that contain both the buffer and the stimulus should be tested and calibrated in order to eliminate any error resulting from pH variation and to best mimic *in vivo* conditions.

It has been shown in neonatal mice that astrocytes from different brain regions exhibit regional heterogeneity in regard to their percentage expression of delta-, kappa-, and mu-opioid receptors (Stiene-Martin et al., 1998). Therefore, it is likely that different spinal regions are also heterogeneous in regard to their opioid receptor expression profiles. In future work, assuming a more equal sample size among spinal and cortical astrocytes, this expression profile heterogeneity should be calculated and utilised when testing astrocytes extracted from different parts of the CNS. In particular, if one is to understand the interactions between any of the different subspecies of opioid receptor and coupled receptors such as P2Y1 for ATP, neurokinin-1 for SP, calcitonin-like

receptor (CL1) and receptor activity-modifying protein 1 (RAMP1) for CGRP, and others one must first know the rate of expression of the receptor in question and then use different opioid receptor agonists such as deltorphin for delta-opioid receptors, DAMGO for mu-opioid receptors like what was used in the current study, and salvinorin A for kappa-opioid receptors.

In general, the results of the current study have affirmed the initial hypothesis that mu-opioid activation in neonatal astrocytes would cause a reduction in the size of calcium responses produced upon stimulation. However, the theory that chronic exposure to DAMGO, as a mu-opioid receptor agonist, would also cause a reduction in the prevalence of stellate astrocytes following exposure to forskolin has been shown to be incorrect. At least with regard to chronic exposure to a single application of DAMGO. If these tests were to be repeated then, firstly, a greater sample size should be used to increase the statistical power of one's findings and, secondly, the astrocytes should be exposed to repeated applications of DAMGO in light of the half-life information presented in the discussion.

References:

Achour, S. Ben, Pont-Lezica, L., Béchade, C., and Pascual, O. (2010). Is astrocyte calcium signaling relevant for synaptic plasticity? Neuron Glia Biol. *6*: 147–155.

Anderson, C.M., Bergher, J.P., and Swanson, R.A. (2004). ATP-induced ATP release from astrocytes. J. Neurochem. *88*: 246–56.

Anderson, D.J. (2000). Genes, lineages and the neural crest: a speculative review. Philos. Trans. R. Soc. B Biol. Sci. *355*: 953–964.

Araque, A., Parpura, V., Sanzgiri, R.P., and Haydon, P.G. (1999). Tripartite synapses: glia, the unacknowledged partner. Trends Neurosci. *22*: 208–15.

Bachoo, R.M., Kim, R.S., Ligon, K.L., Maher, E.A., Brennan, C., Billings, N., et al. (2004). Molecular diversity of astrocytes with implications for neurological disorders. Proc. Natl. Acad. Sci. *101*: 8384–8389.

Bao, L., Jin, S.-X., Zhang, C., Wang, L.-H., Xu, Z.-Z., Zhang, F.-X., et al. (2003). Activation of delta opioid receptors induces receptor insertion and neuropeptide secretion. Neuron *37*: 121–33.

Basbaum, A.I., Bautista, D.M., Scherrer, G., and Julius, D. (2009). Cellular and Molecular Mechanisms of Pain. Cell *139*: 267–284.

Basbaum, A.I., and T, J. (2000). The perception of pain. In Principles of Neuroscience, E.R. Kandel, J. Schwartz, and T. Jessell, Eds. (New York: Appleton and Lange), T. Kandel, E.R.; Schwartz, J; Jessell, ed. (New York: Appleton and Lange), pp 472–491.

Bayraktar, O.A., Fuentealba, L.C., Alvarez-Buylla, A., and Rowitch, D.H. (2015). Astrocyte Development and Heterogeneity. Cold Spring Harb. Perspect. Biol. *7*: a020362.

Bee, L.A., and Dickenson, A.H. (2007). Rostral ventromedial medulla control of spinal sensory processing in normal and pathophysiological states. Neuroscience *147*: 786–793.

Behbehani, M.M., and Fields, H.L. (1979). Evidence that an excitatory connection between the periaqueductal gray and nucleus raphe magnus mediates stimulation produced analgesia. Brain Res. *170*: 85–93.

Ben-Ari, Y., Khalilov, I., Kahle, K.T., and Cherubini, E. (2012). The GABA Excitatory/Inhibitory Shift in Brain Maturation and Neurological Disorders. Neurosci. *18*: 467–486.

Bennett, D.L.H., Averill, S., Clary, D.O., Priestley, J. V., and McMahon, S.B. (1996). Postnatal Changes in the Expression of the trkA High-affinity NGF Receptor in Primary Sensory Neurons. Eur. J. Neurosci. *8*: 2204–2208.

Bessou, P., and Perl, E.R. (1969). Response of cutaneous sensory units with unmyelinated fibers to noxious stimuli. J. Neurophysiol. *32*: 1025–1043.

Blake, A.D., Bot, G., Freeman, J.C., and Reisine, T. (1997). Differential Opioid Agonist Regulation of the Mouse μ Opioid Receptor. J. Biol. Chem. *272*: 782–790.

Bowman, C.L., and Kimelberg, H.K. (1984). Excitatory amino acids

directly depolarize rat brain astrocytes in primary culture. Nature *311*: 656–659.

Burmeister, A.R., Johnson, M.B., Chauhan, V.S., Moerdyk-Schauwecker, M.J., Young, A.D., Cooley, I.D., et al. (2017). Human microglia and astrocytes constitutively express the neurokinin-1 receptor and functionally respond to substance P. J. Neuroinflammation *14*: 245.

Carter, B.D., and Medzihradsky, F. (1993). Go mediates the coupling of the mu opioid receptor to adenylyl cyclase in cloned neural cells and brain. Proc. Natl. Acad. Sci. U. S. A. *90*: 4062–6.

Cassel, J.A., Daubert, J.D., and DeHaven, R.N. (2005). [3H]Alvimopan binding to the μ opioid receptor: Comparative binding kinetics of opioid antagonists. Eur. J. Pharmacol. *520*: 29–36.

Chen, C.-L., Broom, D.C., Liu, Y., Nooij, J.C. de, Li, Z., Cen, C., et al. (2006). Runx1 Determines Nociceptive Sensory Neuron Phenotype and Is Required for Thermal and Neuropathic Pain. Neuron *49*: 365–377.

Chizhmakov, I., Yudin, Y., Mamenko, N., Prudnikov, I., Tamarova, Z., and Krishtal, O. (2005). Opioids inhibit purinergic nociceptors in the sensory neurons and fibres of rat via a G protein-dependent mechanism. Neuropharmacology *48*: 639–647.

Christopherson, K.S., Ullian, E.M., Stokes, C.C.A., Mullowney, C.E., Hell, J.W., Agah, A., et al. (2005). Thrombospondins Are Astrocyte-Secreted Proteins that Promote CNS Synaptogenesis. Cell *120*: 421–433.

Cornell-Bell, A., Finkbeiner, S., Cooper, M., and Smith, S. (1990).

Glutamate induces calcium waves in cultured astrocytes: long-range glial signaling. Science (80-.). *247*: 470–473.

Cronstein, B.N., and Kamen, B.A. (2007). 5-Aminoimidazole-4-Carboxamide-1-β-4-Ribofuranoside (AICA-riboside) as a Targeting Agent for Therapy of Patients With Acute Lymphoblastic Leukemia: Are We There and Are There Pitfalls? J. Pediatr. Hematol. Oncol. *29*: 805–807.

Dani, J.W., Chernjavsky, A., and Smith, S.J. (1992). Neuronal activity triggers calcium waves in hippocampal astrocyte networks. Neuron *8*: 429–440.

Disse, B., Reichl, R., Speck, G., Traunecker, W., Rominger, K.L., and Hammer, R. (1993). Ba 679 BR, A novel long-acting anticholinergic bronchodilator. Life Sci. *52*: 537–544.

Dong, X., Han, S., Zylka, M.J., Simon, M.I., and Anderson, D.J. (2001). A diverse family of GPCRs expressed in specific subsets of nociceptive sensory neurons. Cell *106*: 619–32.

Dou, Y., Wu, H., Li, H., Qin, S., Wang, Y., Li, J., et al. (2012). Microglial migration mediated by ATP-induced ATP release from lysosomes. Cell Res. *22*: 1022–1033.

Eckstein Grunau, R. (2013). Neonatal Pain in Very Preterm Infants: Long-Term Effects on Brain, Neurodevelopment and Pain Reactivity. Rambam Maimonides Med. J. *4*:.

Favero, C.B., and Mandell, J.W. (2007). A pharmacological activator of

AMP-activated protein kinase (AMPK) induces astrocyte stellation. Brain Res. *1168*: 1–10.

Felice, M. De, Eyde, N., Dodick, D., Dussor, G.O., Ossipov, M.H., Fields, H.L., et al. (2013). Capturing the aversive state of cephalic pain preclinically. Ann. Neurol. n/a-n/a.

Finn, A.K., and Whistler, J.L. (2001). Endocytosis of the mu opioid receptor reduces tolerance and a cellular hallmark of opiate withdrawal. Neuron *32*: 829–39.

Fitzgerald, M. (1991). The development of descending brainstem control of spinal cord sensory processing. In Foetal and Neonatal Brainstem: Development and Clinical Issues, M. Hanson, ed. (Cambridge, England: Cambridge University Press), pp 127–36.

Fitzgerald, M. (1993). Development of pain pathways and mechanisms. In Pain in Neonates, K. Anand, and P. McGrath, eds. (New York: Elsevier), pp 19–37.

Fredriksson, R., Lagerström, M.C., Lundin, L.-G., and Schiöth, H.B. (2003). The G-protein-coupled receptors in the human genome form five main families. Phylogenetic analysis, paralogon groups, and fingerprints. Mol. Pharmacol. *63*: 1256–72.

Gardell, L.R., Vanderah, T.W., Gardell, S.E., Wang, R., Ossipov, M.H., Lai, J., et al. (2003). Enhanced evoked excitatory transmitter release in experimental neuropathy requires descending facilitation. J. Neurosci. *23*: 8370–9.

Gauriau, C., and Bernard, J.-F. (2002). Pain pathways and parabrachial circuits in the rat. Exp. Physiol. *87*: 251–8.

Granier, S., Manglik, A., Kruse, A.C., Kobilka, T.S., Thian, F.S., Weis, W.I., et al. (2012). Structure of the δ-opioid receptor bound to naltrindole. Nature *485*: 400–404.

Gray, E.G. (1959). Axo-somatic and axo-dendritic synapses of the cerebral cortex: an electron microscope study. J. Anat. *93*: 420–33.

Haga, K., Kruse, A.C., Asada, H., Yurugi-Kobayashi, T., Shiroishi, M., Zhang, C., et al. (2012). Structure of the human M2 muscarinic acetylcholine receptor bound to an antagonist. Nature *482*: 547–551.

Hamilton, N., Vayro, S., Kirchhoff, F., Verkhratsky, A., Robbins, J., Gorecki, D.C., et al. (2008). Mechanisms of ATP- and glutamate-mediated calcium signaling in white matter astrocytes. Glia *56*: 734–749.

Haydon, P.G., and Nedergaard, M. (2014). How do astrocytes participate in neural plasticity? Cold Spring Harb. Perspect. Biol. *7*: a020438.

Heinricher, M.M., Tavares, I., Leith, J.L., and Lumb, B.M. (2009). Descending control of nociception: Specificity, recruitment and plasticity. Brain Res. Rev. *60*: 214–225.

Hirase, H., Qian, L., Barthó, P., and Buzsáki, G. (2004). Calcium Dynamics of Cortical Astrocytic Networks In Vivo. PLoS Biol. *2*: e96.

Honoré, P., Menning, P.M., Rogers, S.D., Nichols, M.L., Basbaum, A.I., Besson, J.-M., et al. (1999). Spinal Substance P Receptor Expression and Internalization in Acute, Short-Term, and Long-Term Inflammatory

Pain States. J. Neurosci. *19*: 7670–7678.

Hosobuchi, Y., Adams, J.E., and Linchitz, R. (1977). Pain relief by electrical stimulation of the central gray matter in humans and its reversal by naloxone. Science *197*: 183–6.

Hunt, S.P., and Rossi, J. (1985). Peptide- and Non-Peptide-Containing Unmyelinated Primary Afferents: The Parallel Processing of Nociceptive Information. Philos. Trans. R. Soc. B Biol. Sci. *308*: 283–289.

Jamshidi, R.J., Jacobs, B.A., Sullivan, L.C., Chavera, T.A., Saylor, R.M., Prisinzano, T.E., et al. (2015). Functional Selectivity of Kappa Opioid Receptor Agonists in Peripheral Sensory Neurons. J. Pharmacol. Exp. Ther. *355*: 174–182.

Jeremic, A., Jeftinija, K., Stevanovic, J., Glavaski, A., and Jeftinija, S. (2001). ATP stimulates calcium-dependent glutamate release from cultured astrocytes. J. Neurochem. *77*: 664–75.

Kage, K., Niforatos, W., Zhu, C., Lynch, K., Honore, P., and Jarvis, M. (2002). Alteration of dorsal root ganglion P2X 3 receptor expression and function following spinal nerve ligation in the rat. Exp. Brain Res. *147*: 511–519.

Kawasaki, Y., Kumamoto, E., Furue, H., and Yoshimura, M. (2003). Alpha 2 adrenoceptor-mediated presynaptic inhibition of primary afferent glutamatergic transmission in rat substantia gelatinosa neurons. Anesthesiology *98*: 682–9.

Kempski, O., Wroblewska, B., and Spatz, M. (1987). Effects of forskolin

on growth and morphology of cultured glial and cerebrovascular endothelial and smooth muscle cells. Int. J. Dev. Neurosci. *5*: 435–445.

Kim, J.J., Foy, M.R., and Thompson, R.F. (1996). Behavioral stress modifies hippocampal plasticity through N-methyl-D-aspartate receptor activation. Proc. Natl. Acad. Sci. U. S. A. *93*: 4750–3.

King, T., Vera-Portocarrero, L., Gutierrez, T., Vanderah, T.W., Dussor, G., Lai, J., et al. (2009). Unmasking the tonic-aversive state in neuropathic pain. Nat. Neurosci. *12*: 1364–1366.

Kramer, I., Sigrist, M., Nooij, J.C. de, Taniuchi, I., Jessell, T.M., and Arber, S. (2006). A Role for Runx Transcription Factor Signaling in Dorsal Root Ganglion Sensory Neuron Diversification. Neuron *49*: 379–393.

Kruse, A.C., Hu, J., Pan, A.C., Arlow, D.H., Rosenbaum, D.M., Rosemond, E., et al. (2012). Structure and dynamics of the M3 muscarinic acetylcholine receptor. Nature *482*: 552–556.

Kumamoto, E., Mizuta, K., and Fujita, T. (2011). Opioid Actions in Primary-Afferent Fibers—Involvement in Analgesia and Anesthesia. Pharmaceuticals *4*: 343–365.

Liu, W., Tang, Y., and Feng, J. (2011). Cross talk between activation of microglia and astrocytes in pathological conditions in the central nervous system. Life Sci. *89*: 141–146.

Luo, W., Wickramasinghe, S.R., Savitt, J.M., Griffin, J.W., Dawson, T.M., and Ginty, D.D. (2007). A Hierarchical NGF Signaling Cascade Controls Ret-Dependent and Ret-Independent Events during Development of

Nonpeptidergic DRG Neurons. Neuron *54*: 739–754.

Ma, Q., Chen, Z., Barco Barrantes, I. del, la Pompa, J.L. de, and Anderson, D.J. (1998). neurogenin1 is essential for the determination of neuronal precursors for proximal cranial sensory ganglia. Neuron *20*: 469–82.

Ma, Q., Fode, C., Guillemot, F., and Anderson, D.J. (1999). Neurogenin1 and neurogenin2 control two distinct waves of neurogenesis in developing dorsal root ganglia. Genes Dev. *13*: 1717–28.

Manglik, A., Kruse, A.C., Kobilka, T.S., Thian, F.S., Mathiesen, J.M., Sunahara, R.K., et al. (2012). Crystal structure of the μ-opioid receptor bound to a morphinan antagonist. Nature *485*: 321–326.

Marmigère, F., and Ernfors, P. (2007). Specification and connectivity of neuronal subtypes in the sensory lineage. Nat. Rev. Neurosci. *8*: 114–127.

Merskey, H., Albe Fessard, D., Bonica, J., Carmon, A., Dubner, R., Kerr, F., et al. (1979). Pain terms: a list with definitions and notes onusage. Recommended by the IASP subcommittee on taxonomy. Pain *6*: 249–252.

Meyer, R.A., Ringkamp, M., Campbell, J.N., and Raja, S.N. (2008). Peripheral mechanisms of cutaneous nociception. In Textbook of Pain, S.B. McMahon, and M. Koltzenburg, eds. (Philadelphia: Elsevier), pp 3–34.

Molliver, D.C., Wright, D.E., Leitner, M.L., Parsadanian, A.S., Doster, K.,

Wen, D., et al. (1997). IB4-binding DRG neurons switch from NGF to GDNF dependence in early postnatal life. Neuron *19*: 849–61.

Morgello, S., Uson, R.R., Schwartz, E.J., and Haber, R.S. (1995). The human blood-brain barrier glucose transporter (GLUT1) is a glucose transporter of gray matter astrocytes. Glia *14*: 43–54.

Nag, S. (2011). Morphology and Properties of Astrocytes. Methods Mol. Biol. 69–100.

Neary, J.T., Baker, L., Jorgensen, S.L., and Norenberg, M.D. (1994). Extracellular ATP induces stellation and increases glial fibrillary acidic protein content and DNA synthesis in primary astrocyte cultures. Acta Neuropathol. *87*: 8–13.

Nett, W.J., Oloff, S.H., and McCarthy, K.D. (2002). Hippocampal Astrocytes In Situ Exhibit Calcium Oscillations That Occur Independent of Neuronal Activity. J. Neurophysiol. *87*: 528–537.

Norn, S., Kruse, P.R., and Kruse, E. (2005). [History of opium poppy and morphine]. Dan. Medicinhist. Arbog *33*: 171–84.

Oberheim, N.A., Wang, X., Goldman, S., and Nedergaard, M. (2006). Astrocytic complexity distinguishes the human brain. Trends Neurosci. *29*: 547–553.

Olude, M.A., Mustapha, O.A., Aderounmu, O.A., Olopade, J.O., and Ihunwo, A.O. (2015). Astrocyte morphology, heterogeneity, and density in the developing African giant rat (Cricetomys gambianus). Front. Neuroanat. *9*:.

Parri, H.R., Gould, T.M., and Crunelli, V. (2001). Spontaneous astrocytic Ca2+ oscillations in situ drive NMDAR-mediated neuronal excitation. Nat. Neurosci. *4*: 803–812.

Pasternak, G.W. (2014). Opiate Pharmacology and Relief of Pain. J. Clin. Oncol. *32*: 1655–1661.

Perl, E.R. (2007). Ideas about pain, a historical view. Nat. Rev. Neurosci. *8*: 71–80.

Piestrzeniewicz, M.K., Fichna, J., Michna, J., and Janecka, A. (2006). [Opioid receptors and their selective ligands]. Postepy Biochem. *52*: 313–9.

Pinto, M., Sousa, M., Lima, D., and Tavares, I. (2008). Participation of μ-opioid, GABA B , and NK1 receptors of major pain control medullary areas in pathways targeting the rat spinal cord: Implications for descending modulation of nociceptive transmission. J. Comp. Neurol. *510*: 175–187.

Praag, H. van, and Frenk, H. (1991). The development of stimulation-produced analgesia (SPA) in the rat. Brain Res. Dev. Brain Res. *64*: 71–6.

Reynolds, D. V (1969). Surgery in the rat during electrical analgesia induced by focal brain stimulation. Science *164*: 444–5.

Santhappan, R., Crowder, A.T., Gouty, S., Cox, B.M., and Côté, T.E. (2015). Mu opioid receptor activation enhances regulator of G protein signaling 4 association with the mu opioid receptor/G protein complex in

a GTP-dependent manner. J. Neurochem. *135*: 76–87.

Severino, A., Chen, W., Hakimian, J.K., Kieffer, B.L., Gaveriaux-Ruff, C., Walwyn, W., et al. (2018). Mu-opioid receptors in nociceptive afferents produce a sustained suppression of hyperalgesia in chronic pain. Pain *159*: 1607–1620.

Snider, W.D., and McMahon, S.B. (1998). Tackling Pain at the Source: New Ideas about Nociceptors. Neuron *20*: 629–632.

Stiene-Martin, A., Zhou, R., and Hauser, K.F. (1998). Regional, developmental, and cell cycle-dependent differences in mu, delta, and kappa-opioid receptor expression among cultured mouse astrocytes. Glia *22*: 249–59.

Szeto, H.H., Lovelace, J.L., Fridland, G., Soong, Y., Fasolo, J., Wu, D., et al. (2001). In vivo pharmacokinetics of selective mu-opioid peptide agonists. J. Pharmacol. Exp. Ther. *298*: 57–61.

Taati, M., and Tamaddonfard, E. (2018). Ventrolateral orbital cortex oxytocin attenuates neuropathic pain through periaqueductal gray opioid receptor. Pharmacol. Reports *70*: 577–583.

Takasusuki, T., and Yaksh, T.L. (2011). Regulation of Spinal Substance P Release by Intrathecal Calcium Channel Blockade. Anesthesiology *115*: 153–164.

Thomson, L.M., Terman, G.W., Zeng, J., Lowe, J., Chavkin, C., Hermes, S.M., et al. (2008). Decreased Substance P and NK1 Receptor Immunoreactivity and Function in the Spinal Cord Dorsal Horn of

Morphine-Treated Neonatal Rats. J. Pain *9*: 11–19.

Totsuka, Y., Ferdows, M.S., Nielsen, T.B., and Field, J.B. (1983). Effects of forskolin on adenylate cyclase, cyclic AMP, protein kinase and intermediary metabolism of the thyroid gland. Biochim. Biophys. Acta *756*: 319–27.

Trafton, J.A., Abbadie, C., Marchand, S., Mantyh, P.W., and Basbaum, A.I. (1999). Spinal opioid analgesia: how critical is the regulation of substance P signaling? J. Neurosci. *19*: 9642–53.

Troadec, J.D., Thirion, S., Petturiti, D., Bohn, M.T., and Poujeol, P. (1999). ATP acting on P2Y receptors triggers calcium mobilization in primary cultures of rat neurohypophysial astrocytes (pituicytes). Pflugers Arch. *437*: 745–53.

Vanegas, H., and Schaible, H.-G. (2004). Descending control of persistent pain: inhibitory or facilitatory? Brain Res. Rev. *46*: 295–309.

Vortherms, T.A., and Roth, B.L. (2005). Receptorome screening for CNS drug discovery. IDrugs *8*: 491–6.

Vulchanova, L., Riedl, M.S., Shuster, S.J., Stone, L.S., Hargreaves, K.M., Buell, G., et al. (1998). P2X 3 is expressed by DRG neurons that terminate in inner lamina II. Eur. J. Neurosci. *10*: 3470–3478.

Won, C.-K., and Oh, Y.S. (2000). cAMP-induced stellation in primary astrocyte cultures with regional heterogeneity. Brain Res. *887*: 250–258.

Wu, H., Wacker, D., Mileni, M., Katritch, V., Han, G.W., Vardy, E., et al. (2012). Structure of the human κ-opioid receptor in complex with JDTic.

Nature *485*: 327–332.

Xu, G.-Y., and Huang, L.-Y.M. (2002). Peripheral Inflammation Sensitizes P2X Receptor-Mediated Responses in Rat Dorsal Root Ganglion Neurons. J. Neurosci. *22*: 93–102.

Xue, J.C., Chen, C., Zhu, J., Kunapuli, S.P., Riel, J.K. De, Yu, L., et al. (1995). The third extracellular loop of the μ opioid receptor is important for agonist selectivity. J. Biol. Chem. *270*: 12977–12979.

Yoon, H., Walters, G., Paulsen, A.R., and Scarisbrick, I.A. (2017). Astrocyte heterogeneity across the brain and spinal cord occurs developmentally, in adulthood and in response to demyelination. PLoS One *12*: e0180697.

Yoshikawa, M., Senzaki, K., Yokomizo, T., Takahashi, S., Ozaki, S., and Shiga, T. (2007). Runx1 selectively regulates cell fate specification and axonal projections of dorsal root ganglion neurons. Dev. Biol. *303*: 663–674.

Zimmerman, D.M., Leander, J.D., Reel, J.K., and Hynes, M.D. (1987). Use of beta-funaltrexamine to determine mu opioid receptor involvement in the analgesic activity of various opioid ligands. J Pharmacol Exp Ther *241*: 374–378.